geosciences

MDPI

Article

Pre-Orogenic Tectonostratigraphic Evolution of the European Distal Margin-Alpine Tethys Transition Zone in High-Pressure Units of the Southwestern Alps

Gianni Balestro [1,*], Andrea Festa [1,2], Paola Cadoppi [1], Chiara Groppo [1] and Matthieu Roà [1]

[1] Department of Earth Sciences, University of Torino, Via Valperga Caluso 35, 10125 Torino, Italy
[2] National Research Council of Italy, Institute of Geosciences and Earth Resources, Via Valperga Caluso 35, 10125 Torino, Italy
* Correspondence: gianni.balestro@unito.it

Abstract: Geological mapping, stratigraphic observations, and U/Pb dating allow reconstructing the pre-orogenic setting of the transition zone between the distal European passive margin and the Alpine Tethys in the southwestern Alps. Although convergent tectonics overprinted the syn-rift Jurassic tectonic features, our data document an articulated Jurassic physiography. From the distal European passive margin oceanward, we distinguished: the Dronero Unit (the southernmost Dora Maira massif), represents a continental margin composite basement wherein monometamorphic metasediments are interlayered with Late Permian (253.8 ± 2.7 Ma) metavolcanic rocks; the Sampeyre Unit, represents a structural high consisting of Lower Triassic Verrucano-facies siliciclastic metasediments unconformably sealed by Cretaceous calcschist bearing *Globotruncana* sp.; the Maira Unit, corresponds to a Middle Triassic platform succession detached from the Sampeyre Unit; the Grana Unit, corresponds to a Late Triassic–Late Jurassic platform to basin succession; the Queyras Schistes Lustrès Complex, represents the ocean basin succession. Tectonic slices of Cambrian (513.9 ± 2.7 Ma) metadiorite hosted in the Valmala Shear Zone, separating the Dronero Unit from the underlying (U)HP units of the Dora Maira massif, suggests a potential pre-Alpine activation of the shear zone.

Keywords: ocean-continent transition zone; structural inheritance; tectonostratigraphy; Dora Maira massif; Western Alps

Citation: Balestro, G.; Festa, A.; Cadoppi, P.; Groppo, C.; Roà, M. Pre-Orogenic Tectonostratigraphic Evolution of the European Distal Margin-Alpine Tethys Transition Zone in High-Pressure Units of the Southwestern Alps. *Geosciences* **2022**, *12*, 358. https://doi.org/10.3390/geosciences12100358

Academic Editors: Olivier Lacombe and Jesus Martinez-Frias

Received: 19 August 2022
Accepted: 23 September 2022
Published: 27 September 2022

1. Introduction

The Alps are the most studied orogen in the world and a natural laboratory wherein models related to orogenic building are currently developed and improved. Models focused on mechanisms causing the formation of collisional belts [1] increasingly take into account the role of inherited (i.e., pre-Alpine) structures in controlling orogenic architectures [2,3]. In the Western Alps, paleogeographic and tectonic reconstructions significantly rely on structural inheritances arising from rifted margin and oceanic lithosphere architectures [4–8], and from basement/cover or platform/basin transitions [9–11]. These inheritances have indeed an important role in controlling subduction initiation and collision processes [12–14].

Since Alpine-related tectonics strongly overprint the pre-Alpine structures and crustal architectures, the study of pre-Alpine structures has to be focused on low strain domains, wherein the effects of deformation and metamorphism are less pervasive [15]. This is the case of a sector of the southwestern Alps, wherein remnants of the Permian-Triassic pre-rift and Jurassic syn-rift successions occur (Figure 1). After the key works of Vialon (1966) [16] and Michard (1967) [17], this sector was poorly investigated although in the Western Alps, it is the only one wherein an almost complete section of the transition between the distal European margin and the Alpine Tethys is partly preserved [18].

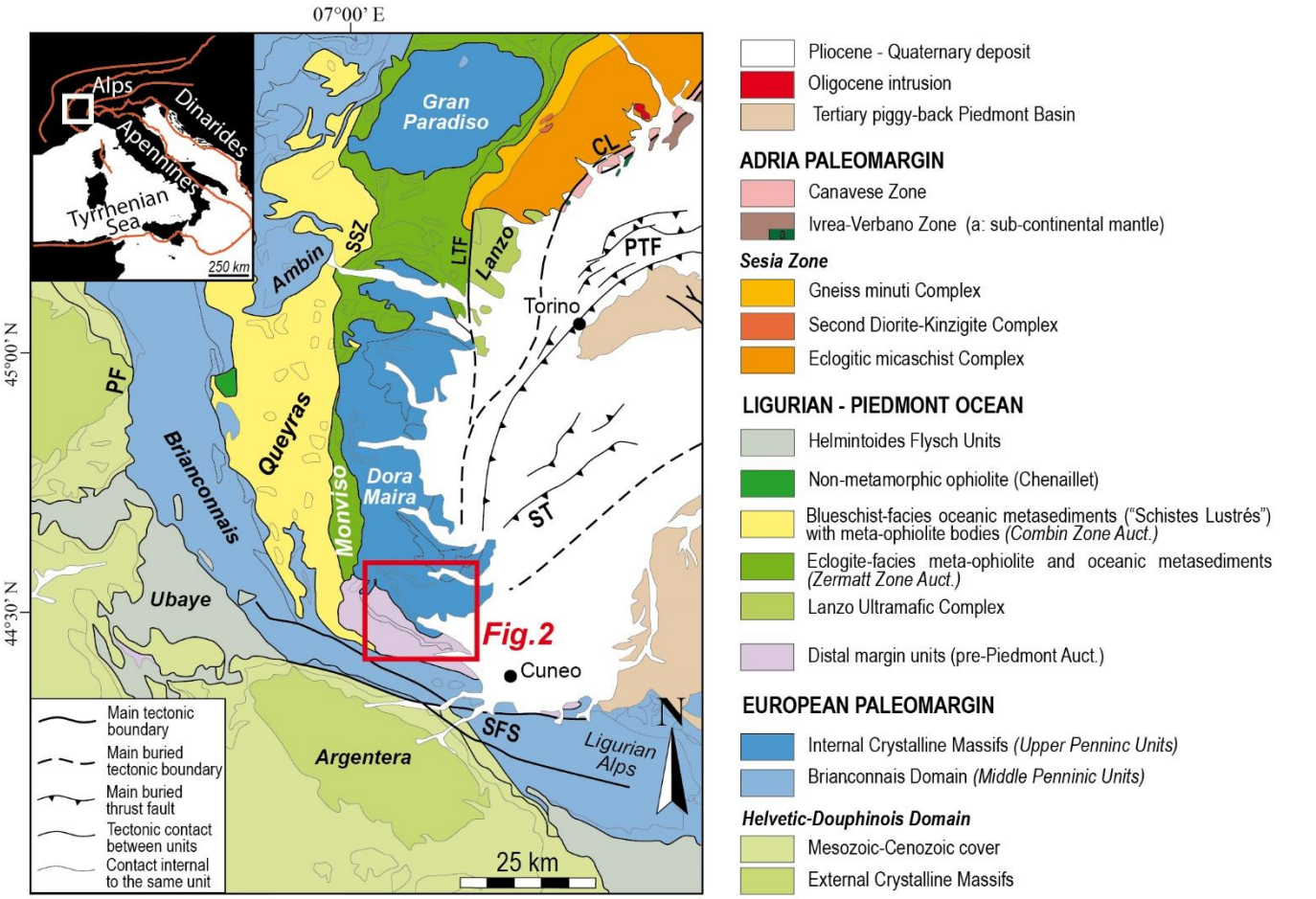

Figure 1. Simplified tectonic map of the Western Alps showing the location of the study area (red square). CL, Canavese Line; PF, Penninic Front; PTF, Padane Thrust Front; ST, Saluzzo Thrust; SFS, Stura Fault System; SSZ, Susa Shear Zone; LTF, Lis-Trana Fault.

In this paper, through data reviewing and new chronostratigraphic data, we describe in detail the lithostratigraphies of the superposed tectonostratigraphic units in the inner southwestern Alps. This allowed us to reconstruct the pre-Alpine tectonostratigraphic setting of the transition between the distal European passive margin and the Alpine Tethys, as documented in other sectors of the Alps [19,20]. We document the existence of an articulated pre-Alpine tectonic setting of the margin, with inherited faults and structural highs and lows, and the importance of the role of inherited structures in constraining the development of Alpine shear zones and basement/cover detachments at different lithostratigraphic levels.

2. Geological Setting

The tectonic evolution of Western Alps resulted from the Cenozoic convergence between Europe and Adria and was influenced by a complex inherited paleogeography, such as the Mesozoic crustal architecture. The latter was characterized by a major Tethyan seaway (i.e., the Jurassic-Cretaceous Ligurian-Piedmont Ocean Basin; LPOB hereafter) interposed between the Briançonnais European micro-continent and the Adria African promontory [21–24]. The Western Alpine orogenic belt formed through (i) Late Cretaceous to Middle Eocene subduction, (ii) Late Eocene to Oligocene continental collision and deep crust/mantle indentation, and (iii) Neogene strike-slip and extensional tectonics [25–28]. During these three geodynamic stages, the axial sector of the belt grew up as a double verging accretionary wedge [29–31], involving terranes derived from the Adria (i.e., the Austroalpine units) and Europe (i.e., the Penninic units) paleomargins and from the

LPOB [32] (i.e., the Piedmont Zone). Alpine tectonic units have been characterized by different PTt trajectories, and they are progressively less deformed and metamorphosed from inner eastern to external western sectors of the axial belt [33,34].

In the southwestern sector of the axial belt (Figure 1), different tectonic units derived from the paleo-European continental crust and passive margin, and from LPOB, have been distinguished [35,36]. These tectonic units form a complex nappe stack wherein carbonate metasedimentary successions [17,37] (i.e., the pre-Piedmont Auct.) and oceanic units of the Piedmont Zone [8,38–42] (i.e., the Monviso meta-ophiolite and Queyras Schistes Lustrès complexes) are tectonically interposed in between continental crust units of the Dora Maira Massif [43] and Briançonnais Domain [44]. Due to late Alpine hinterland-verging folding and backthrusting [45], units of the Internal Briançonnais Domain overlie the Queyras Schistes Lustrès Complex.

The Dora-Maira Massif (DMM hereafter) is a slab of European crust likely sourced from the more distal sector of Briançonnais micro-continent [8], and it now corresponds to a composite stack of units [16,46–48]. These units consist of pre-Carboniferous basement rocks, Lower Permian magmatic bodies, and Upper Carboniferous to Triassic metasediments [49–54]. The lowermost unit exposed in the Pinerolo tectonic window was metamorphosed under blueschist-facies metamorphic conditions [55,56] and in the southern sector of the DMM, was overthrusted by different eclogite-facies (San Chiaffredo and Rocca Solei) and coesite eclogite-facies (Brossasco-Isasca) units [57–61]. The latter units are in turn tectonically overlain by the blueschist-facies Dronero and Sampeyre units [62–64].

The Internal Briançonnais (IBD hereafter) and the External Briançonnais domains derive from the Briançonnais microcontinent, which is thought to had been located between the Valaisan basin and LPBO [65]. Compared to the DMM, the IBD was less affected by Alpine tectonometamorphic processes. In the southwestern Alps, two main units [66–68] (i.e., the Acceglio and Grum units) of IBD tectonically overlie the Queyras Schistes Lustrès Complex. They are mainly made up of Permian volcanic rocks and Early Triassic siliciclastic metasediments, with minor slices of Jurassic carbonate metasediments, and were metamorphosed under low- to high-grade blueschist-facies conditions [69].

The southwestern sector of the axial belt (Figure 1) is characterized by widespread carbonate metasedimentary successions, which are detached from their basements (the Maira-Sampeyre and Val Grana Allochthons of Michard et al., 2022 [36]) and derive from the transition zone between the European distal margin and the LPBO [69]. These successions were indicated as pre-Piedmont units [37] and, based on paleontological relicts, they are constrained in age between the Triassic and Jurassic [17,70–72]. The pre-Piedmont succession mainly consists of metadolostone, marble, and carbonate-rich calcschist overlain by detrital complexes of calcschist and carbonate metabreccia and olistoliths [17].

The Piedmont Zone encompasses the remnants of the LPBO sampled in the orogeny wedge and in the southwestern Alps, consists of the southern termination of the Monviso meta-ophiolite Complex [5,73,74] and of the overlying Queyras Schistes Lustrès Complex (QSLC hereafter). The latter consists of meta-ophiolite blocks that are embedded in an oceanic metasedimentary succession [38]. Blocks are made up of serpentinized metaperidotite, metagabbro, metabreccia with mafic–ultramafic clasts, and metabasalt [38,75], whereas the metasedimentary succession mainly consists of Middle Bathonian to Late Oxfordian metachert, Tithonian to Berriasian marble, and Cretaceous calcschist [76,77]. As well as in the Monviso meta-ophiolite Complex [78], in the QSLC findings of ocean-related structures and oceanic core complexes, architectures have been described [40,41]. During Alpine tectonics, the QSLC was dismembered into tectonometamorphic units [79,80], whose metamorphic conditions range between low temperature to high temperature blueschist-facies [81,82].

3. Methods

The lithostratigraphic successions and the present day tectonic stack have been detected through geological mapping carried out at 1:10,000 scale, using common techniques

of field mapping. Petrographic and microfossil data have relied on both mesoscale observations and optical microscope analysis. U–Pb geochronology was carried out using a Resonetics RESOlution M-50 series 193 nm excimer laser ablation system equipped with a Laurin Technic Pty S-155 ablation cell. Details about instrumental conditions are reported in Supplementary Materials (Tables S1 and S2).

4. Tectono-Stratigraphic Setting

The present day tectono-stratigraphic setting of the inner southwestern Alps consists of the tectonic stack of five main tectonostratigraphic units (Figure 2; [83]), which are separated by major shear zones. These units represent the remnants of (i) the distal European passive margin (i.e., the Dronero, Sampeyre and Maira units), (ii) the transition zone between the margin and the LPBO (i.e., the "pre-Piedmont" Grana Unit), and (iii) the LPBO (i.e., the QSLC of the Piedmont Zone), differing for the characteristics of the lithostratigraphic succession.

The tectonic stack is bounded at the top and bottom by the tectonic contact with the IBD and the eclogite-facies DMM units, respectively, whose description is out of the aim of this paper. In the following (Sections 4.1–4.3), the tectonostratigraphic units are described by focusing on primary (i.e., pre-Alpine) contacts and on the reconstruction of stratigraphic successions that, despite the Alpine deformation and metamorphic overprint, can be recognized in the study area. Chronostratigraphic constraints are provided by remnants of fossils, which are described in the following, and by U–Pb geochronology (see Section 5). Ages of protoliths are referred to the geological timescale of the International Chronostratigraphic Chart by Cohen et al. (2013, updated) [84].

4.1. The Distal European Passive Margin Succession

The stratigraphic succession of the distal European passive margin outcrop in three tectonostratigraphic units (i.e., the Dronero, Sampeyre units, and Macra Unit), which differ in the structural position within the orogenic stack and the lithostratigraphic characteristics (Figure 2).

4.1.1. The Dronero Unit

The Dronero Unit (Dronero *Ensemble* [16]; DU hereafter) represents the lowermost tectonostratigraphic unit (Figure 2). It is bounded at the base by the Valmala Shear Zone [85] (VSZ hereafter), along which it is juxtaposed to the Brossasco-Isasca and Rocca Solei units (Figure 2). The up to several hundreds of meters-thick VSZ consists of tectonically juxtaposed lenticular slices of metadiorite, garnet- and chloritoid-bearing mylonitic micaschist, mylonitic augen gneiss, quartz-rich mylonitic schist and quartzite, and marble). The VSZ also includes discontinuous slices of massive serpentinite, carbonate-bearing serpentine schist, mylonitic metabasite, and mylonitic calcschist. Among the lithologies of these tectonic slices, a metadiorite sample has been selected for U/Pb dating (see Section 5.1).

The DU is characterized by a composite lithostratigraphic succession (Figure 3A), consisting of a polymetamorphic basement (i.e., rocks metamorphosed during both the Variscan and Alpine orogenic cycles), and of monometamorphic metaintrusives and metasediments (i.e., rocks metamorphosed only during the Alpine orogenic cycle) [49,62,85]. The polymetamorphic basement mainly consists of coarse-grained garnet- and chloritoid-bearing micaschist (Figure 3B) with relics of Variscan staurolite and garnet in the mineral assemblage [57]. The micaschist locally hosts meter-sized bodies of metabasite and levels of quartzite. Monometamorphic metaintrusive rocks mainly consists of K-feldspar bearing coarse- to medium-grained augen gneiss (Figure 3C) derived from several hundreds of meters-sized granite and tonalite bodies. Medium-grained leucogneiss and orthogneiss of granodioritic composition also occur.

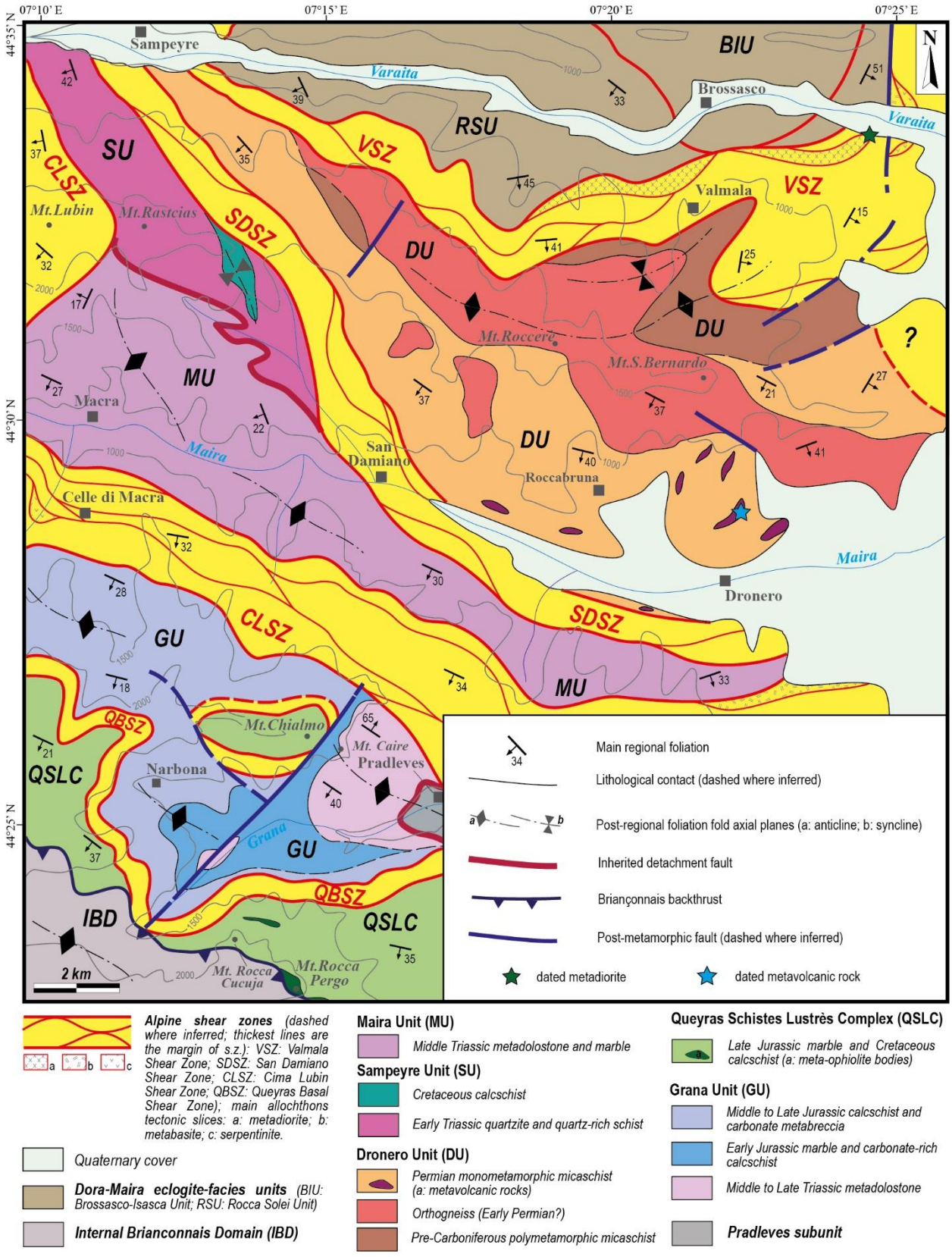

Figure 2. Geological map of the study area in the Western Alps, showing the spatial and tectonic relationships of tectonostratigraphic units.

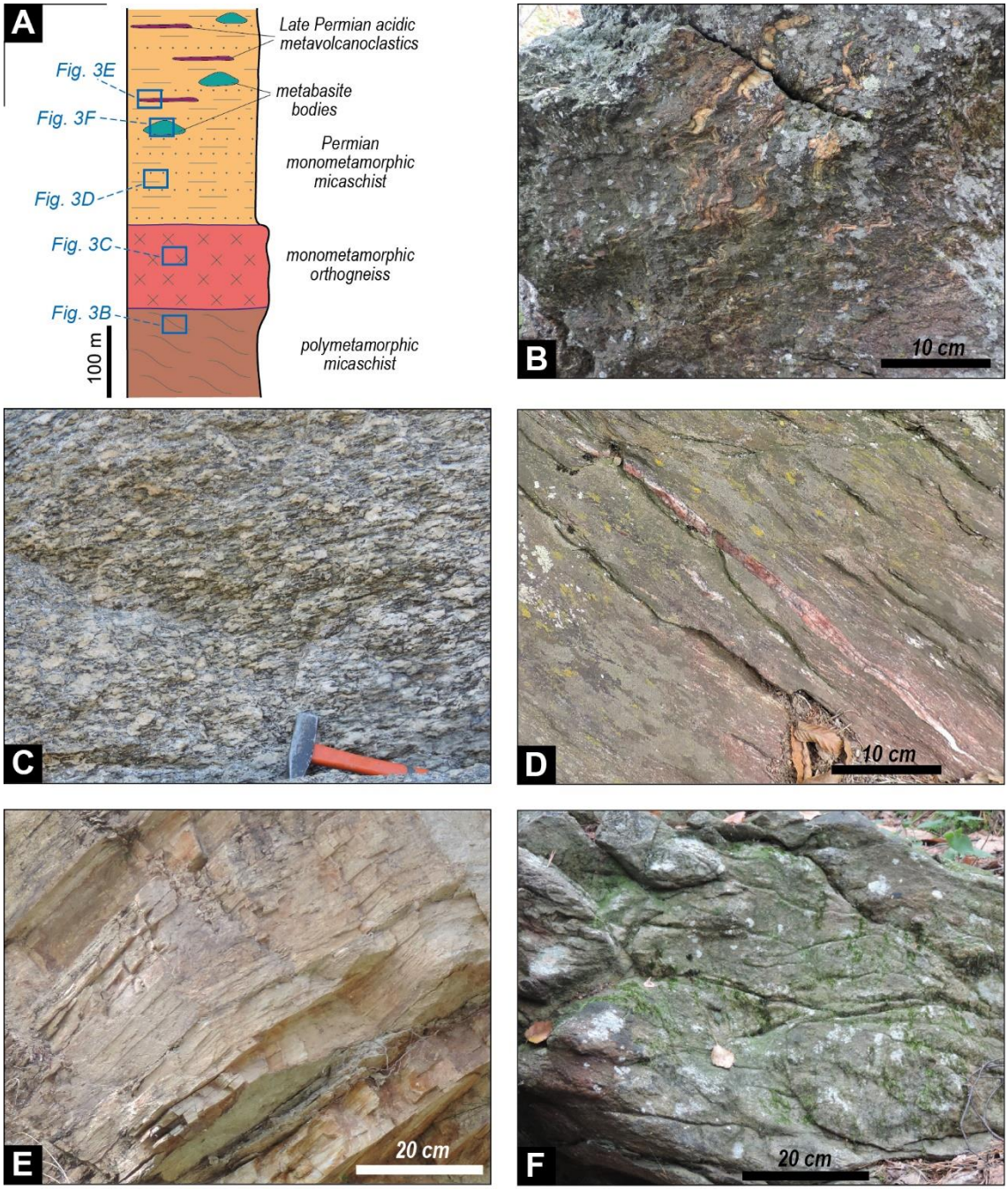

Figure 3. (**A**) Pre-Alpine stratigraphic columnar section of the Dronero Unit (the stratigraphic location of the representative field images is shown); (**B**) close-up view of the polymetamorphic micaschist (South of Valmala); (**C**) close-up view of the monometamorphic metagranitoid (West of Mt. S.Beranardo); (**D**) close-up view of the Permian monometamorphic micaschist (North of Dronero); (**E**) view of the outcrop of micro-augen gneiss selected for U/Pb dating (North of Dronero); (**F**) close-up view of a metabasite body with nodular texture hosted in the monometamorphic micaschist (North of Dronero).

The monometamorphic metasediments consist of greyish fine-grained micaschist (Figure 3D), varying from garnet- and/or chloritoid-bearing micaschist to quartz-rich micaschist and albite-rich micaschist, hundreds of meters in thickness, locally alternating with micaceous quartzite and graphite-bearing micaschist horizons, up to a few meters thick. Metasediments are locally characterized by intercalations of micro-augen gneiss

layers, up to several meters in thickness. This gneiss is medium-grained and greyish to whitish in color (Figure 3E), and it shows a mineral assemblage characterized by K-feldspar porphyroclasts, up to several millimeters in size, which are embedded in a fine-grained matrix mainly consisting of quartz, albite, and white mica, with minor epidote, biotite, apatite, and zircon. The textural relics and mineral assemblage suggest that the augen gneiss derives from poorly reworked volcaniclastic layers of acidic composition, which emplaced in the metasedimentary succession, now represented by the above described micaschists.

Massive to pervasively foliated metabasite bodies (Figure 3F), up to few meters thick and locally characterized by centimeters to decimeters rounded nodules of epidosite, are also interlayered within the metasediments. The metabasite is fine to medium-grained and greenish in color, and shows relics of porphyritic texture, which is defined by tabular to prismatic aggregates mainly consisting of epidote and amphibole, and epidote and white mica, likely replacing phenocrysts of pyroxene and plagioclase, respectively. These aggregates are embedded in a very fine-grained matrix consisting of epidote, chlorite, amphibole, albite, biotite, white mica, and quartz. The textural relics and the mineral assemblage suggest that the metabasite derives from volcanic rocks of mafic- to intermediate-composition.

The monometamorphic metasediments can be attributed to the Permian Period, mainly because of (i) the lack of Variscan-related mineral relics, and (ii) their stratigraphic position above the polymetamorphic basement and below the detached Mesozoic successions (i.e., the Sampeyre and Maira units). One of the metavolcanic horizons interlayered in these metasediments, has been here selected for U/Pb dating to better constrain this age (see Section 5.2).

4.1.2. The Sampeyre Unit

The Sampeyre Unit (Sampeyre *Ensemble* [16]; SU hereafter) is bounded at the base by a several hundreds of meters-thick shear zone (the San Damiano Shear Zone [36]; SDSZ hereafter; Figure 2). The latter consists of tectonic slices wrenched from the DU and SU successions, but it also embeds lenticular bodies of metadolostone and marble sourced from the carbonate succession of the Maira Unit (see Section 4.1.3).

The SU consists of a siliciclastic metasedimentary succession locally overlain by carbonate metasediments (Figure 4A). It shows lateral thickness variations, with a maximum thickness of about few hundreds of meters, tapering out toward SE (Figure 2).

The siliciclastic metasediments consist of quartz-rich schist and quartzite. The former is light grey in color, medium-grained, and pervasively foliated, with a mineral assemblage mainly characterized by quartz, chloritoid, and minor garnet, albite, chlorite, amphibole, epidote, and carbonate. The quartz rich schist turns upward into pale green poorly foliated white mica-bearing quartzite and massive thick-bedded white quartzite. These two rock types are interpreted as deriving from a quartz-rich conglomerate. The mineral assemblage also consists of minor carbonate, chlorite, and albite. In the massive quartzite, sedimentary textures are partially preserved and defined by (i) whitish to pinkish clasts of quartz (Figure 4B), and (ii) rare K-feldspar porphyroclasts. This succession corresponds to the "Werfenian quartzites" [47] and can be compared to the *Ponte di Nava Quartzite*, which represents the upper part of the Late Permian–Early Triassic Briançonnais Verrucano [86] in the Ligurian Alps (i.e., the southeastern prosecution of the Briançonnais Domain; Figure 1). Comparable siliciclastic metasediments also occur in the IBD successions [66], where their top has been referred to the Olenekian Stage based on local vertebrate footprints [87].

Through a well preserved primary lithostratigraphic contact (i.e., devoid of any mylonitic structure), the siliciclastic metasediments are locally overlain by calcschist, up to few tens of meters in thickness. The calcschist (Figure 4C) is commonly greyish in color and fine- to medium-grained. The mineral assemblage mainly consists of calcite, white mica, and quartz, with minor dolomite, ankerite, chlorite, and Fe-oxides. Remarkably, very fine-grained aggregates of calcite and Fe-oxide (Figure 4D–F) document remnants of planktonic Foraminifera (i.e., *Globotruncana* species). These remnants, which were never described before in the study area, are well-comparable with those locally described in

other calcschists of the Western Alps [88–90] and mostly referred to the lower part of the Upper Cretaceous, suggesting that the calcschist succession unconformably deposited above the Late Permian–Early Triassic deposits.

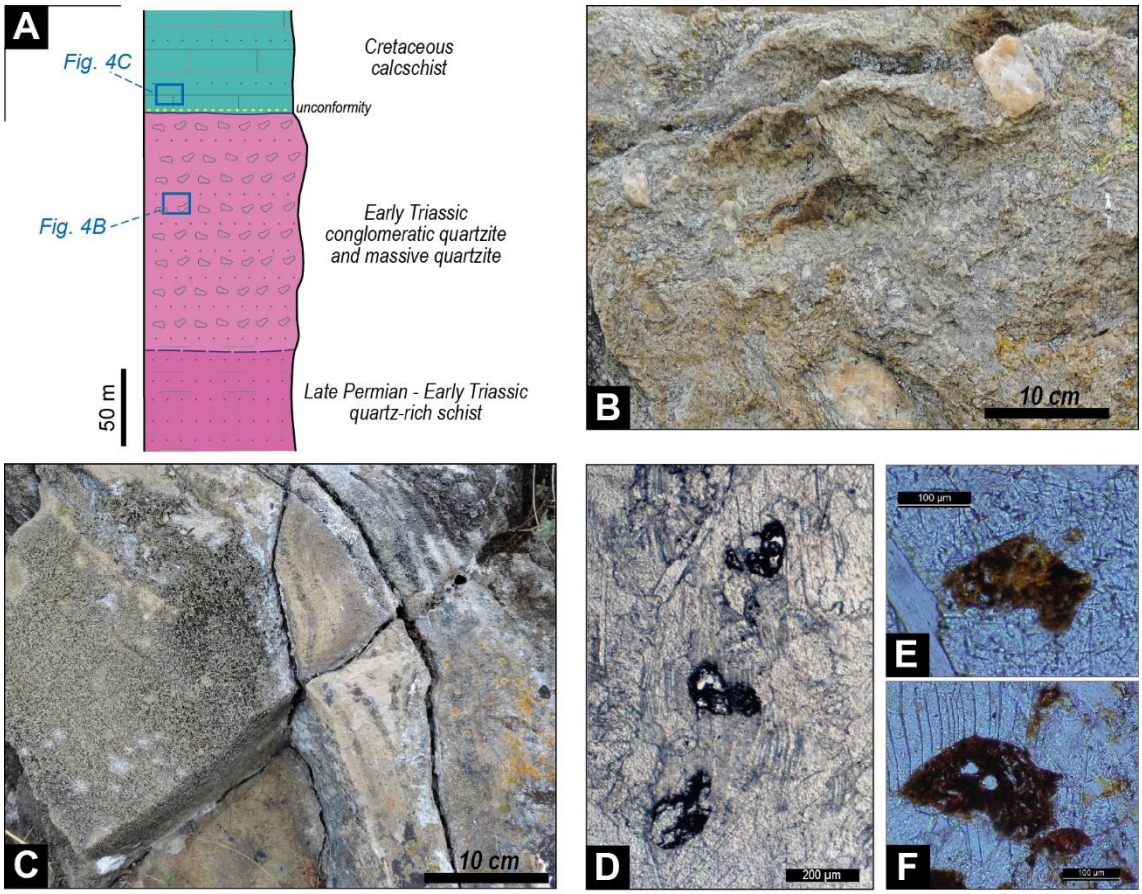

Figure 4. (**A**) Pre-alpine stratigraphic columnar section of the Sampeyre Unit (the stratigraphic location of the representative field images is shown); (**B**) close-up view of the Early Triassic conglomeratic quartzite with centimers-sized clasts of quartz (South-East of Mt.Rastcias); (**C**) close-up view of the Cretaceous calcschist bearing Globotruncana sp., which stratigraphically overlies the quartzite (South-East of Mt.Rastcias); (**D**–**F**) thin section images (plane polarized ligh) of the calcschist of Figure 4C, including aggregates of calcite and Fe-oxide replacing planktonic Foraminifera (i.e., *Globotruncana* sp.).

4.1.3. The Maira Unit

The Maira Unit (MU hereafter) corresponds to the Trias *Calcaro-Dolomitique* [17], and consists of metadolostone and marble, up to several hundreds of meters in thickness, and thinning toward SE. In the sector wherein the SU does not occur, the MU is directly juxtaposed to the DU through the SDSZ (Figure 2). Differently from other shear zones, the tectonic contact between SU and MU is (i) pervasively folded, (ii) limited in thickness (i.e., from several meters to few tens of meters), and (iii) it mainly consists of mylonitic marble, pervasively fractured quartzite, and tectonic carbonate breccia.

The lower part of the MU succession (Figure 5A) is characterized by yellowish metadolostone (Figure 5B), vuggy metadolostone, and dolomitic marble. They mainly consist of dolomite and calcite, with minor ankerite, white mica, and pyrite. Local cavernous textures likely result from dissolution/recrystallization processes of primary evaporite (Anisian?) as also suggested by rare findings of gypsum levels within the succession [71].

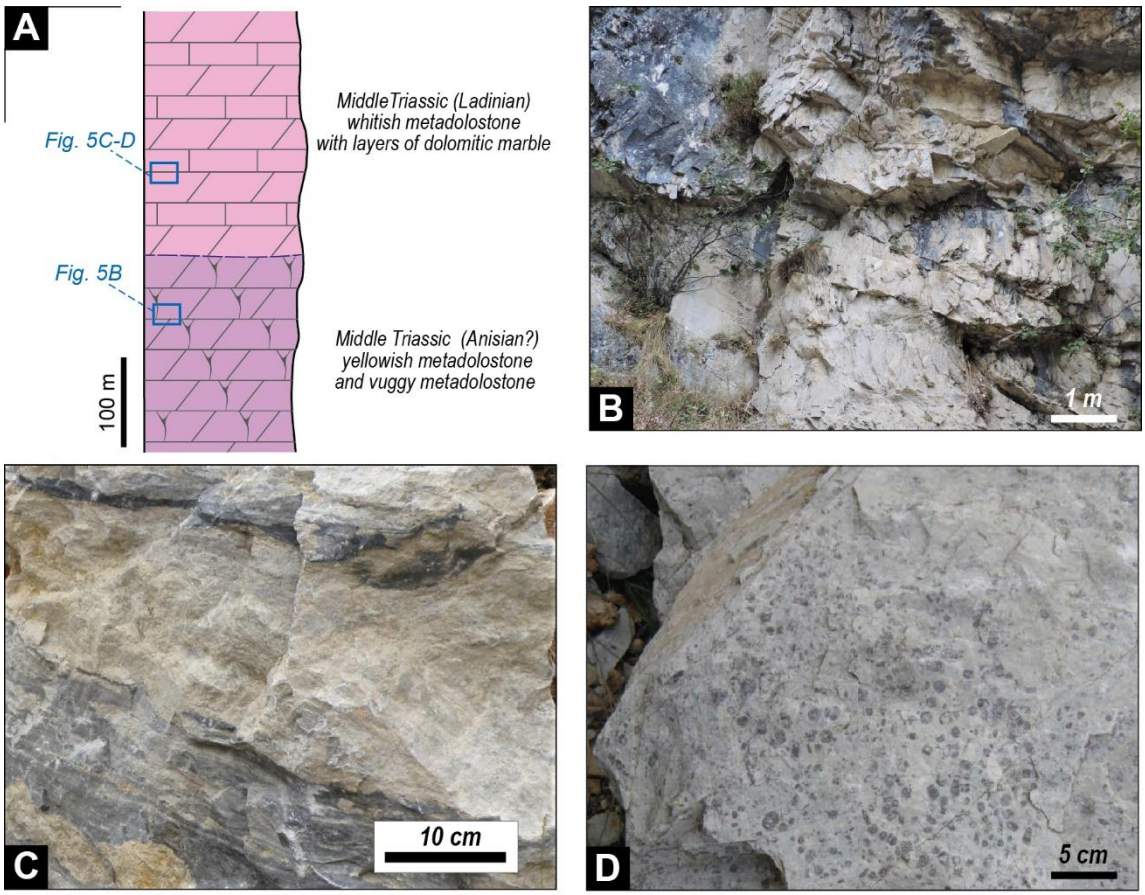

Figure 5. (**A**) Pre-Alpine stratigraphic columnar section of the Maira Unit (the stratigraphic location of the representative field images is shown); (**B**) (Anisian?) yellowish metadolostone (North-East of San Damiano); (**C**) close-up view of the Ladinian whitish metadolostone alternating with layers of grey dolomitic marbles (South of Dronero); (**D**) close-up view of the Ladinian whitish metadolostone retaining fragments of crinoids (South of Dronero).

The MU succession continues upward with whitish and massive metadolostone (Figure 5A), which is fine grained and mainly consists of dolomite with minor sub-millimeters white mica-bearing levels. The metadolostone is locally alternating with layers of dolomitic marble (Figure 5C), consisting of calcite, dolomite, ankerite, and with mica, with minor quartz and pyrite, and with rare centimeter to decimeter-thick interlayers of blackish schist, deriving from very fine-grained anoxic layers. The metadolostone is also locally interbedded with decimeter-thick horizons of pale brownish to pale greenish dolomite-bearing calcschist, which has been interpreted as original tuffite beds emplaced during carbonate sedimentation [17].

Recrystallized fragments of crinoids (Figure 5D), dasycladacean algae, and gastropods (details about faunas) [17,71] allowed dating the whitish and massive metadolostone to the Ladinian age. The stratigraphic characteristics of the MU is well comparable with those of the *San Pietro dei Monti Dolomite* [91] in the Ligurian Alps, which in fact is referred to the Ladinian age based on the paleontological content (details in Vanossi, 1969, [91], and Decarlis and Lualdi, 2008 [92]).

4.2. The Transitional Zone Succession

The transition zone between the distal European passive margin and the LPBO (Figure 6A) consists of a single tectonostratigraphic unit (i.e., the Grana Unit; GU hereafter) thinning toward NW (Figure 2), which corresponds to the pre-Piedmont Auct. [37]. It records the stratigraphic transition between the Late Permian–Middle Triassic dis-

tal European margin succession and the Jurassic–Cretaceous oceanic succession of the Alpine Tethys.

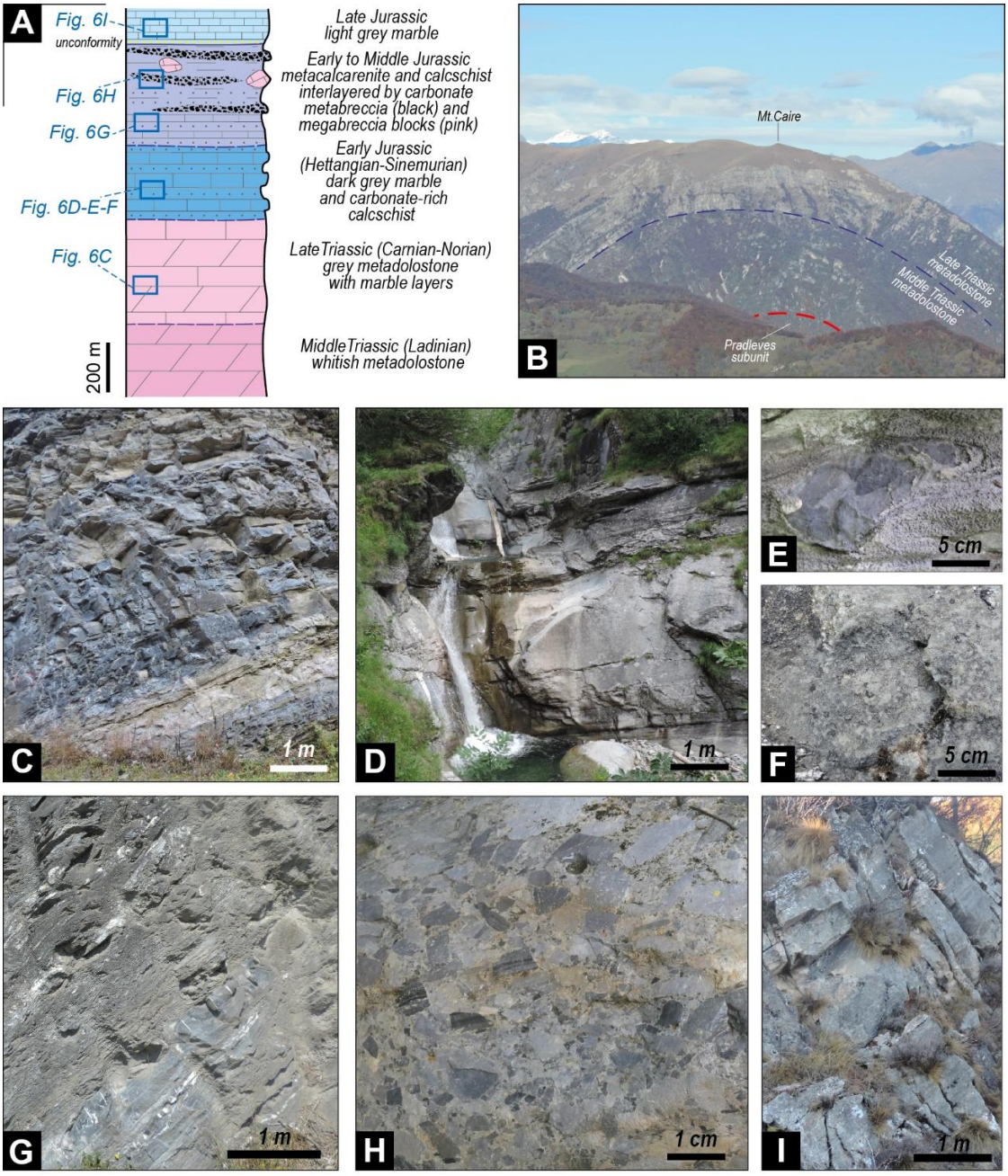

Figure 6. (**A**) Pre-Alpine stratigraphic columnar section of the Grana Unit (the stratigraphic location of the representative field images is shown); (**B**) panoramic view of the Pradleves anticline deforming the lower part of the GU succession and the underlying Pradleves subunit (dashed blue line: contact between the Ladinian metadolostone and the Carnian-Norian metadolostone; dashed red line: tectonic contact between the GU and the Pradleves subunit); (**C**) view of the Carnian-Norian cyclic carbonate metasediments consisting of alternating banded metadolostone and marble layers (South-East of Narbona, along the Grana river); (**D**) view of the ammonite-bearing Sinemurian marble and carbonate-rich calcschist (South-East of Narbona); (**E**,**F**) close-up views of remnants of recrystallized and partly deformed ammonites (South-East of Narbona); (**G**) view of the alternating Early to Middle Jurassic marble and calcschist (East of Narbona); (**H**) close-up view of an Early to Middle Jurassic poorly matrix-supported metabreccia consisting of angular clasts of metadolostone and marble in a carbonate matrix (Narbona); (**I**) view of the Late Jurassic light grey marble (South of Celle di Macra).

The GU is bounded by a one-kilometer-thick shear zone, which is the thickest one of the studied sector, and corresponds to the southeastern continuation of the Cima Lubin Shear Zone (CLSZ hereafter) [36]. The CLSZ consists of up to a kilometer-long and hundreds of meter-thick tectonic slices, which were wrenched both from SU, MU, and GU successions. Slices of serpentinite and of metabasite also occur (Figure 2).

The Grana Unit

The lower part of the GU succession consists of tens of meters-thick dark grey fetid metadolostone passing upward to roughly two hundreds of meters-thick whitish and massive metadolostone, which is texturally and mineralogically comparable with the above described Ladinian metasediments of MU succession. Differently from the latter, GU better preserves its paleontological content (i.e., recrystallized fragments and remnants of crinoids, dasycladacean algae, gastropods, foraminifera, and rare ammonoid cephalopods; details in Michard, 1967 [17] and Michard and Sturani, 1963 [93]). It is worth to point out that, in the Pradleves area, the metadolostone tectonically rests above conglomeratic quartzite, which in turn stratigraphically overlies micaschist with bodies of metabasite (i.e., the Pradleves subunit in Figure 2). The tectonic contact between GU and the Pradleves subunit, similarly to that between MU and SU, is folded (i.e., the Pradleves anticline; Figure 6B) and defined by several meters-thick tectonic carbonate breccia and mylonitic metadolostone.

The GU succession continues upward to cyclic carbonate metasediments (Figure 6C), up to four hundreds of meters in thickness, consisting of alternating very fine-grained banded metadolostone, mainly grey in color, and marble layers, mainly made up of calcite with minor dolomite, white mica, and quartz. Recrystallized fragments and remnants of Dasycladacean algae, gastropods, ostracods, and bivalves (details in Michard, 1967 [17] and Franchi and Di Stefano, 1896, [94]), allowed dating this lithostratigraphic unit to the Carnian-Norian age. A comparison with part of the Norian *Monte Arena Dolomite* [95], which represents a peri-to-subdital deposit, is suggested.

The succession continues upward with three hundreds of meters thick marble, which can be divided into a lower and an upper part. The former consists of banded, fine-grained, dark grey marble locally alternating with decimeters thick metadolostone layers. Recrystallized fragments of gastropods and lamellibranches, allowed Franchi (1898) [71] dating these rocks to the Rhaetian-Hettangian age. The upper part consists of medium-grained marble with nodular beds, and of carbonate-rich grey calcschist (Figure 6D), made up of different amounts of calcite, quartz, and white mica, with minor chlorite, epidote, and albite. This upper marble is characterized by three biostratigraphic levels with remnants of ammonites (Figure 6E,F) and belemnites. These three levels have been attributed to the base, the lower and upper parts of Sinemurian age (details in Sturani, 1961, [72], and Ellenberger et al., 1964 [96]).

The upper part of the GU succession consists of up to three hundreds of meters-thick alternating metacalcarenite, grey marble, and calcschist with discontinuous quartz layers (Figure 6G), which are both interlayered by different horizons of carbonate metabreccia and megabreccia blocks (i.e., olistoliths and olitoliths fields). The bottom of this part of the GU succession corresponds to the *Calcaires de la Bercia* of Michard [17], which have been attributed to the Pliensbachian age based on their stratigraphic position above the late Sinemurian metasediments. This age attribution also agrees with the age of the *Rocca Livernà* Limestone (Early Hettangian–Pliensbachian–Toarcian(?)), described by Boni et al. (1971) [95] and Decarlis and Lualdi (2011) [97] in the Ligurian Alps, even if, in contrast with the Calcaire de la Bercia, significant breccia layers are lacking.

The metabreccia horizons are mainly decimeter-thick and consist of poorly matrix-supported angular clasts of Carnian-Norian metadolostone and Rhaetian-Hettangian marble [17,72], embedded in a scanty grey-blackish calcite matrix (Figure 6H). The megabreccia (i.e., olistoliths field), roughly occurs in the same stratigraphic position of metabreccia horizons, and mainly consists of meter-sized rounded to lenticular metadolostone, grey metadolostone, and yellowish dolomitic marble with cavernous texture blocks. Meter-wide blocks

of quartzite with quartz micro-clasts have also been described [98]. The age of these blocks is well comparable with that of the above described metabreccia clasts. The metabreccia can be referred, except for the lack of blocks of the Paleozoic basement and of the volcanic sequence, to the *Monte Galero Breccia* of the Prepiedmont Units of the Ligurian Alps [95,99], whose age span is between the upper part of Lower Jurassic and the lower part of Middle Jurassic.

The uppermost part of the GU succession consists of (i) calcschist interbedded by horizons of quartz-rich schist and (ii) tabular light grey marble (Figure 6I), up to fifty meters in thickness. This marble, which can be tentatively referred to the Late Jurassic (see also Michard et al., 2022 [36]), is anyway mostly detached from the underlying Early to Middle Jurassic lithostratigraphic units of the GU succession and partially sliced along the shear zone that separates the GU from the QSLC (see below).

4.3. The Ocean Basin Succession

The LPBO succession (Figure 7A) outcrops in the southeastern sector of the QSLC [100], which is separated from the GU through the Queyras Basal Shear Zone (QBSZ hereafter; Figure 2). The latter shows a maximum thickness of about few hundreds of meters and consists of mylonitic calcschist embedding tectonic slices of serpentinite, metabasite and marble, and blocks of metadolostone. These blocks are almost transformed into tectonic carbonate breccia and distributed parallel to the margin of the shear zone (i.e., the *coussinet tectonique* of Michard, 1961 [83]). The QSLC is in turn overthrust by the IBD. Further description of this tectonic contact is out of the aim of the paper.

The Queyras Schistes Lustrès Complex

The QSLC consists of calcschist embedding lenticular bodies of metaophiolite and continuous horizons of marble. The calcschist consists of interlayered by decimeter-thick light brown to grey carbonate-rich layers and dark grey carbonate-poor and graphite-rich layers (Figure 7B), about decimeters in thickness. The mineral assemblage is made up of calcite, white mica, quartz, and graphite, with minor chlorite, ankerite, and opaque minerals and textural relics of lawsonite. This calcschist has been generically referred to the Early Cretaceous and to the earliest Late Cretaceous [17,100] by comparison with the *Palombini* Shale of the non-metamorphosed cover of the Internal Ligurian ophiolites in the Northern Apennines [40,101]. The rounded and lenticular bodies of metaophiolite, up to few hundreds of meters in size, locally preserve terms of the primary oceanic "complete" successions, consisting of serpentinite, metagabbro, mafic/ultramafic metabreccia, metabasalt, metachert, and marble [40,41,102,103].

The serpentinite is mainly massive and medium-grained, with rare textural relics of the primary peridotite assemblage, and mostly consists of serpentine and magnetite, with minor talc, amphibole, and chlorite. The metagabbro ranges from Mg-Al to Fe-Ti-rich composition, and occurs as both dykes and up to decameter-wide masses with massive textures. The Mg-Al metagabbro is coarse-grained and retains primary textural relics (Figure 7C), with aggregates of albite, zoisite, and clinozoisite grown on sites of magmatic plagioclase, and aggregates of omphacite, amphibole, albite, and epidote replacing magmatic pyroxene. The Fe-Ti metagabbro is medium-grained and is mainly made up of omphacite, amphibole, albite, chlorite, epidote, titanite, and rutile. The metagabbro is also locally crosscut by metadolerite dykes. The mafic/ultramafic metabreccia rarely occurs as few meters-thick horizons, stratigraphically overlying the serpentinite and metagabbro. It corresponds to the first sedimentary layers originally deposited on seafloor exhumed mantle rocks [103]. The metabreccia is commonly poorly sorted, and mostly consists of centimeter-sized clasts of serpentinite and metagabbro embedded in a matrix made up of calcite, amphibole, and chlorite.

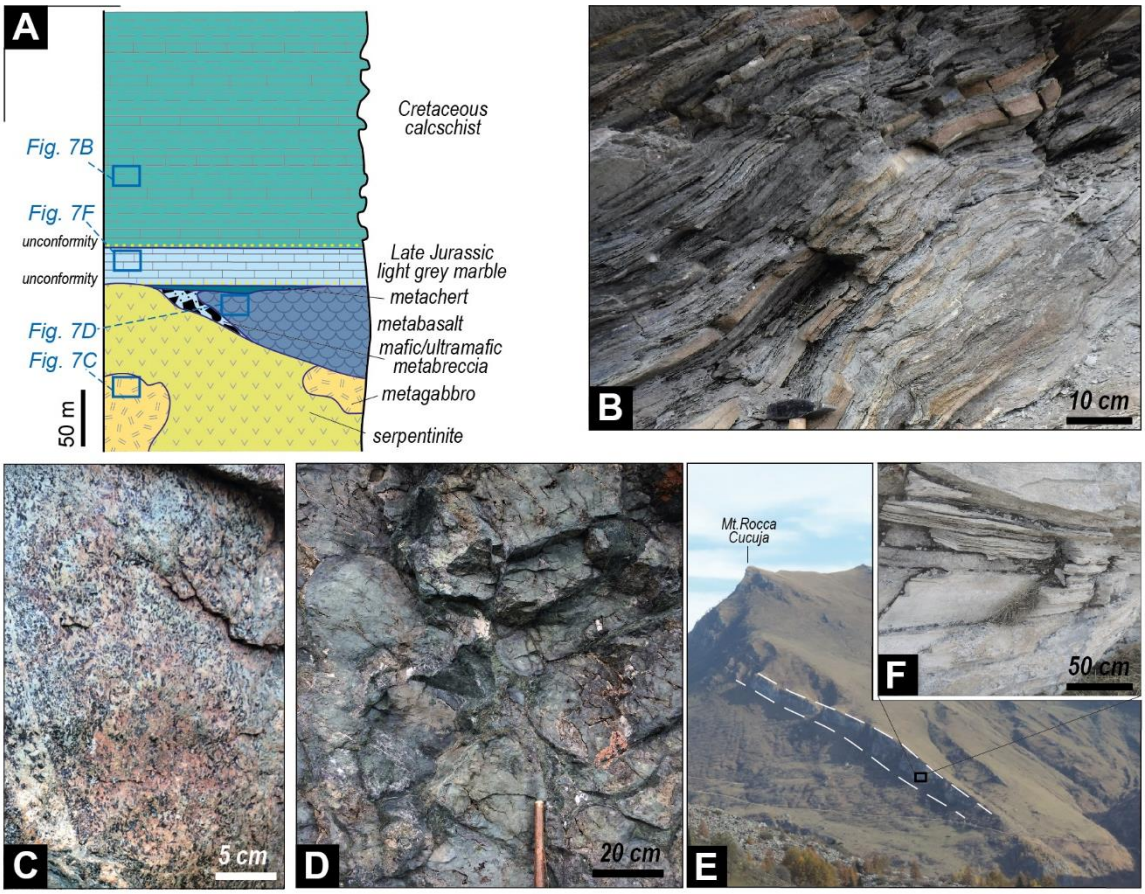

Figure 7. (**A**) Pre-Alpine stratigraphic columnar section of the Queyras Schistes Lustrès Complex (the stratigraphic location of the representative field images is shown); (**B**) Cretaceous calcschist consisting of interlayered light brown carbonate-rich and dark grey carbonate-poor layers (North-East of Mt.Rocca Cucuja); (**C**) massive coarse-grained metagabbro of Mg-Al rich composition mainly consisting of dark grey pyroxene and greenish white plagioclase (Mt. Rocca Pergo); (**D**) metabasalt retaining pillow-breccia structures (Mt. Rocca Pergo); (**E**) panoramic view of a tabular body (dashed white lines) of Late Jurassic whitish marble within the calcschist; (**F**) close-up view of the massive whitish marble and of the more foliated carbonate-rich calcschist.

The metabasalt, up to tens of meters in thickness, were originally emplaced both above the serpentinite and metagabbro, and above mafic/ultramafic metabreccia. It mainly corresponds to banded metabasite, which often retains magmatic textures consisting of decimeters-sized pillow and pillow-breccia structures (Figure 7D). Its mineral assemblage is made up of albite, amphibole, chlorite, epidote, white mica, stilpnomelane, and calcite. The metabasalt is locally overlain, or interlayered close to its top, by banded metachert. The latter is up to few meters in thickness, fine-grained and greyish in color, and mainly consists of quartz, with minor white mica and opaque minerals.

In the meta-ophiolite bodies, the serpentinite and metagabbro or the metabasalt and metachert are overlain and or wrapped, at least in part, by meter-thick horizons of fine-grained tabular whitish to grey marble. The latter is mostly made up of calcite, with minor quartz, amphibole, white mica, ankerite, and opaque minerals. A similar tabular marble, grading to light grey carbonate-rich calcschist, occurs within the calcschist as tabular bodies (Figure 7E,F), which are up to several tens of meters in thickness and lateral continuous along a few kilometers [18]. This marble shows a close facies similarity with the Late Jurassic uppermost part of the GU succession.

Although radiometric ages from magmatic rocks of the meta-ophiolite bodies are not available in the study area, metachert west of the study area (i.e., the Traversiera

Massif, [104]) retains radiolarian microfossils early referred to the Late Oxfordian–Early Kimmeridgian age [104] and then revised to Late Bathonian–Early Callovian age (UAZ 7) [105,106]. The age of the whitish and tabular marble is constrained to the upper part of the Late Jurassic to the earliest part of the Early Cretaceous [107] by correlation with the *Calpionella* Limestone of the non-metamorphosed cover of the Internal Ligurian ophiolites in the Northern Apennines [101].

5. U–Pb Geochronology

U–Pb dating of zircons has been carried out from two samples, a metadiorite from VSZ and a metavolcanite from DU, in order to detect their magmatic ages. Results of U–Pb dating are given in the following. Details about analyses and instrumental conditions are reported in Supplementary Materials (Tables S1 and S2).

5.1. U–Pb Dating of the Metadiorite from the Valmala Shear Zone

The metadiorite (sample 204) has been sampled ENE of Valmala locality (right side of the Varaita River Valley; Long. 7°24′25″, Lat. 44°33′39″; Figure 2). The metadiorite is massive and contains decimeter-sized mafic enclaves and highly transposed (i.e., few decimeters thick but hundreds of meters long) acidic dykes (Figure 8A,B). The mineral assemblage consists of albite, blue and green amphibole, clinozoisite, and chlorite, with minor garnet, quartz, white mica, titanite, ilmenite, rutile, and zircon.

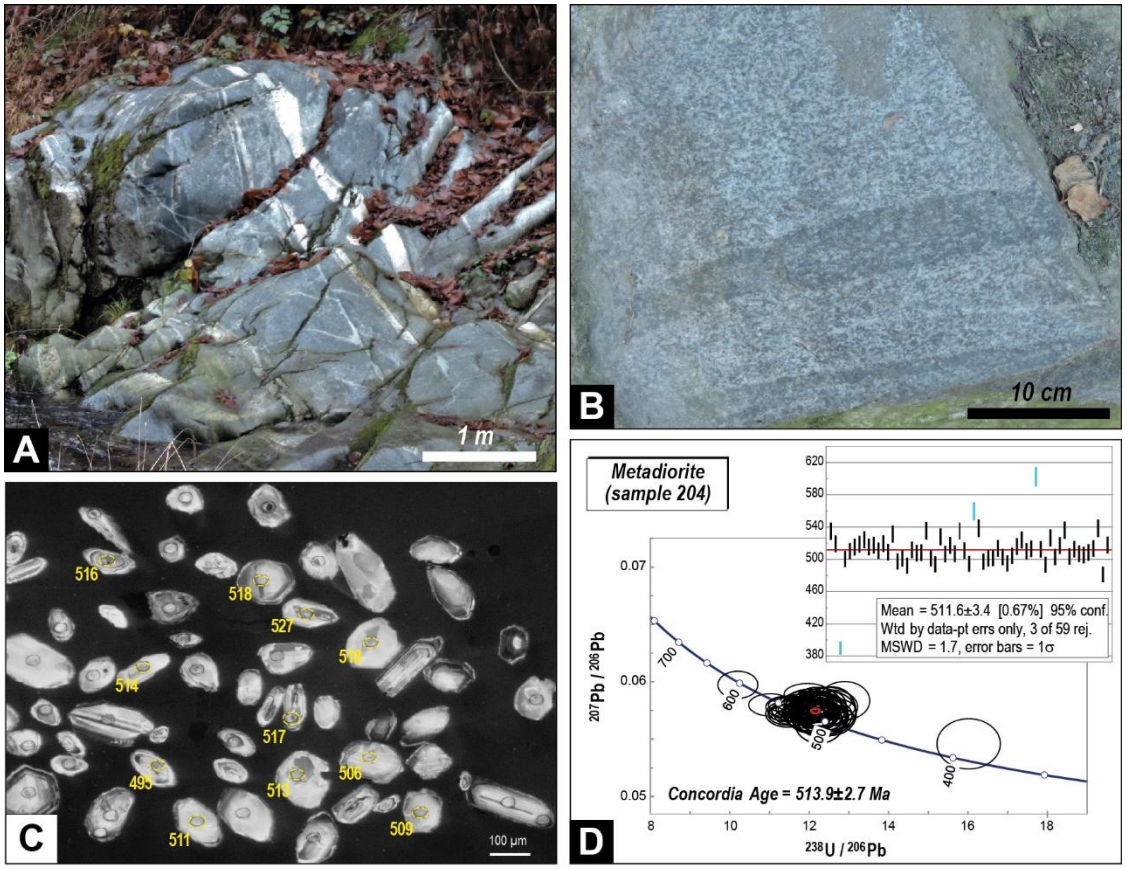

Figure 8. (**A**) View of the metadiorite with acidic dykes (N of Valmala); (**B**) close-up view of the outcrop of the metadiorite with a mafic enclave selected for U/Pb dating (ENE of Valmala); (**C**) CL image of some of the analyzed zircon grains (measured spots are shown by yellow circles with related ages); (**D**) concordia Tera–Wasserburg ($^{207}Pb/^{206}Pb$ vs. $^{238}U/^{206}Pb$) and weighted average ($^{206}Pb/^{238}U$ ages) diagrams for analyzed zircons (sample 204).

Result of U/Pb analyses are detailed in the Supplementary Table S1. Fifty-nine laser ablation analyses were carried out on the core of fifty-six zircon crystals, consisting of subhedral colorless crystals (50–200 µm in size) partly characterized by magmatic oscillatory zoning (Figure 8C). $^{206}Pb/^{207}Pb$ and $^{238}U/^{206}Pb$ ratios have been plotted in a Tera–Wasserburg diagram and are almost concordant, yielding a concordia age of 513.9 ± 2.7 Ma (weighted average age = 511 ± 3.4 Ma; MSWD = 1.7; Figure 8D), corresponding to the magmatic age of the diorite. U/Pb dating thus highlights that Cambrian intrusive rocks were tectonically sampled along the VSZ. It is here remarked that meta-intrusive rocks with comparable composition and age, have never been reported in the units surrounding the VSZ. The potential geological meaning of this occurrence of Cambrian metadiorite is discussed in the following (Section 6.3).

5.2. U–Pb Dating of the Metavolcanics from the Dronero Unit

The metavolcaniclastic horizon (sample 1920) has been sampled North of Dronero locality (left side of the Maira River Valley; Long. 7°21′53″, Lat. 44°28′50″; Figure 2). The sample contains millimeters-sized K-feldspar porphyroclasts embedded in a fine-grained matrix mainly consisting of quartz, albite, and white mica, with minor epidote, biotite, apatite, and zircon.

Analytical methods and result of U/Pb dating are reported in the Supplementary Table S2. Euhedral to subhedral zircon grains are clear, colorless, and 50–200 µm in size, with magmatic oscillatory zoning, and a magmatic high-temperature type morphology [108]. Fifty-two laser ablation analyses were carried out on the core of forty-eight zircon crystals (Figure 9A). $^{206}Pb/^{207}Pb$ and $^{238}U/^{206}Pb$ ratios have been plotted in a Tera–Wasserburg diagram and are almost concordant, yielding a concordia age of 253.8 ± 2.7 Ma (weighted average age = 253.8 ± 2.0 Ma; MSWD = 1.8; Figure 9B). Since the metavolcaniclastic layers can be considered as nearly coeval with the hosting metasediments [109], the U/Pb dating roughly constrains the age of monometamorphic metasediments protolith of the DU succession to the Lopingian Epoch (i.e., Late Permian).

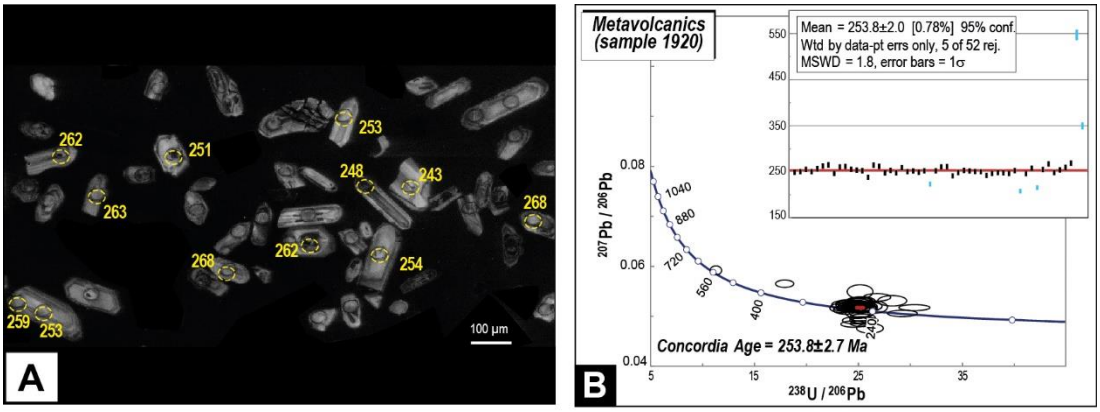

Figure 9. (**A**) CL image of some of the analyzed zircon grains (measured spots are shown by yellow circles with related ages); (**B**) concordia Tera–Wasserburg ($^{207}Pb/^{206}Pb$ vs. $^{238}U/^{206}Pb$) and weighted average ($^{206}Pb/^{238}U$ ages) diagrams for analyzed zircons (sample 1920).

6. Discussion

The reconstruction of the structural setting of the southern part of the Western Alps, allowed to distinguish tectono-stratigraphic units that preserve different portions of the primary transition between the LPBO and the European passive margin. The stratigraphic characteristics and facies variation within each tectono-stratigraphic unit allow reconstructing in detail of the pre-orogenic tectonic evolution, which can be subdivided in two main stages (Sections 6.1 and 6.2). The overall inherited (i.e., pre-Alpine) tectonostratigraphic setting and structural architecture is discussed in Section 6.3.

6.1. Permian to Triassic Continental Lithosphere Extension

This stage is recorded in DU, SU, and MU successions. Although these units are tectonically separated through SDSZ, their stratigraphic successions allow defining a continuous record of Middle Permian–Middle Triassic sedimentation.

The characteristics of the polymetamorphic basement of DU, which mainly consists of garnet- and chloritoid-bearing micaschist, are comparable with those of the polymetamorphic basement described in the southern DMM [61] (i.e., in the Brossasco-Isasca and Rocca Solei units) in which different metagranitoid bodies [62] have been dated as Guadalupian (i.e., Middle Permian; ~275 Ma, [58]; ~262 Ma, [110]). The monometamorphic basement consisting of different types of micaschist, interlayered with bodies of metabasite derived from mafic- to intermediate tuffites, and with acidic meta-volcaniclastic rocks [108], suggests pyroclastic eruptions [111,112] in a continental environment. U/Pb dating constrains metavolcanic rocks to the Lopingian Epoch (i.e., Late Permian; ~255 Ma), indirectly dating the hosting metasediments. This age documented for the first time in the DMM and is well-comparable with the ~258 Ma age of K-alkaline rhyolite within the Permian continental successions from the Briançonnais domain in the Ligurian Alps [113]. According to the reconstructed evolution of the Ligurian Alps [86], the metavolcanic rocks likely represent the product of large-scale lithospheric extension (i.e., the second magmatic cycle of Cortesogno et al., 1998 [114]), which took place after widespread calc-alkaline volcanic activities (i.e., the first magmatic cycle of Cortesogno et al., 1998 [114]) associated with the Early Permian transtensional tectonics and collapse of the Variscan belt [115]. In the DMM, differently from the Briançonnais Domain, the Early Permian magmatism was characterized by emplacement of intrusive bodies [50] rather than by volcanic activity.

The Late Permian magmatism was associated with variation in the thermal state of the lithosphere and widespread extensional and transtensional tectonics [24,116]. Extension lasted until the Triassic and controlled the development of Late Permian–Early Triassic WNW-trending graben basins [86], wherein Verrucano clastic sediments deposited. The characteristics of siliciclastic metasediments of SU, consisting of quartz-rich schist and quartzite, are well-comparable with the Briançonnais Verrucano, representing the Late Permian–Early Triassic deposition of a fluvio-deltaic succession of sand, siltstone, well-sorted arkose, and conglomerates as also documented in different sector of the Alpine-Mediterranean region [117]. The depositional contact with the Permian sediments and volcanic rocks, which corresponds to a regional scale unconformity, is not exposed because SU is tectonically separated from DU by SDSZ.

The unconformable deposition of the Upper Cretaceous calcschist protoliths, preserving remnants of planktonic foraminifera (*Globotruncana* sp.), on Verrucano deposits (i.e., the stratigraphic contact between siliciclastic and carbonate metasediments) outlines that SU represented a structural/morphological high up to Late Cretaceous as discussed in the following (Section 6.3). On the contrary, the occurrence in MU of a complete Anisian (i.e., vuggy metadolostone and dolomitic marble with local occurrence of cavernous texture resulting from dissolution/recrystallization processes of primary evaporite) to Ladinian (i.e., metadolostone comparable with the Ladinian *San Pietro dei Monti Dolomite* [91] in the Ligurian Alps) succession, documents the onset of platform carbonate sedimentation in the sector represented by this unit.

The lack of terms younger than the Ladinian metadolostone does not allow to completely understand if MU was a sector of relative structural/morphological high or of low. Its present-day structural position between the structural/morphological high of the SU and the GU succession, which represents a structural/morphological low, tentatively suggests that MU corresponded to a sector of connection between SU and GU. In the GU, in fact, the Ladinian metadolostone turns in a cyclic peri- to sub-tidal Carnian–Norian succession (i.e., comparable with the *Monte Arena Dolomite* [95]) of alternating very fine-grained banded metadolostone and marble, which are in turn followed by a complete and fossil-rich Early Jurassic succession.

At the regional scale, the deposition of the Middle to Late Triassic platform successions was linked to a widespread subsidence resulting from lithospheric cooling after the Permian thermal event [118]. Evidence of extensional tectonics in the Briançonnais and Prepiedmont domains of the Ligurian Alps, are provided by syn-sedimentary normal faults in the *San Pietro dei Monti Dolomite* [86].

6.2. Jurassic Ocean Spreading

This stage, related to the opening of the Alpine Tethys, is recorded in the fossil-rich succession of GU, whereas on the contrary of DU, SU, and MU consists of an almost complete Late Triassic–Late Jurassic platform to basin succession. This succession differs from the typical Briançonnais successions, which emerged and was eroded during Late Triassic to Early Jurassic regional uplift [92]. The depositional environment in which the GU succession deposited was affected by a continuous subsidence with respect to the European continental margin (i.e., DU, SU, and MU). A first rifting stage has been referred to the deposition of Norian Monte Arena Dolomite [86], but the main tectonic input (i.e., the second rifting stage of Decarlis et al., 2013 [86]) is recorded in Early–Middle Jurassic by the carbonate metabreccia horizons and megabreccia or olistolith fields (i.e., the *Complexe Détritique* of Lemoine, 1971 [119]), triggered by mass-wasting processes along faults scarps. Composition and facies of clasts and olistoliths constrain their source from the tectono-gravitational dismemberment of the pre-Pleinsbachian carbonate platform successions.

In the Prepiedmont units of the Ligurian Alps, two main sub-stages have been distinguished within the second rifting stage [86]: the first one was characterized by activation of extensional and strike-slip faults followed by fast subsidence (i.e., the deposition of the Early Jurassic *Rocca Livernà Limestone*); the second sub-stage corresponds to the margin collapse with detrital deposition along active fault scarps (i.e., the Early–Middle Jurassic *Monte Galero Breccia*).

Remnants of the ocean spreading-related tectonics also occur in the meta-ophiolite bodies of the QSLC, which however are tectonically embedded within the Lower- to Upper Cretaceous calcschist (i.e., the former Late Cretaceous-Paleocene accretionary prism; [120]). These bodies preserve, in fact, different portions of the mantle-cover oceanic lithosphere succession, recording the seafloor spreading of a restricted oceanic basin (i.e., the LPBO) from the Middle Jurassic [121,122] to the Late Jurassic–Early Cretaceous [40].

In GU, the upper temporal constraint to the ocean spreading stage is represented by the uppermost part of the GU succession, consisting of the Upper Jurassic tabular marble. The close similarity of this marble with the Upper Jurassic massive carbonate-rich calcschist and marble occurring as elongated bodies in the QSLC succession, suggests an original lateral facies transition between GU and QSLC.

6.3. The Inherited (Pre-Alpine) Structural Architecture

The Late Triassic to Middle Jurassic stratigraphic successions, ranging from reduced (i.e., SU and MU) to complete (i.e., GU and the successions within the meta-ophiolite bodies of the QSLC), clearly documented the role played by active extensional tectonics in forming an articulated tectono-stratigraphic depositional environment at the transition between the European distal margin and LPBO (Figure 10). Although convergent tectonics reworked, overprinted, and masked in large part the primary tectonic features that controlled sedimentation, they likely corresponded to extensional to transtentional faults as extensively documented in other sectors of the Western Alps [7,20,123].

Evidence that the Upper Permian–Lower Triassic Verrucano-facies metasediments of SU were unconformably sealed by the Upper Cretaceous calcschist bearing Globotruncana sp., clearly indicates that the inherited Late Triassic to Middle Jurassic architecture locally characterized portions of the European distal margin–Alpine Tethys transition zone up to Early Cretaceous and/or the beginning of Late Cretaceous. The MU and SU successions are juxtaposed through a deformation zone that, differently from the other shear zones, is pervasively folded and thinner. This deformation zone is characterized by tectonic

carbonate breccia and may represent a reactivated extensional fault that controlled sedimentation and formation of a structural high, as also Michard et al. (2022) [36] suggested. A similar tectonic contact occurs in the Pradleves sector of GU, separating the quartzite of the Pradleves subunit from the above metadolostone and localized at the base of the carbonate platform succession. It is not excluded that both the contacts between MU and SU and between the Pradleves subunit and GU represent the remnants, at a margin-scale, of a same (inherited) fault system. The latter could be structurally linked with a main extensional detachment fault, which likely drove the exhumation of the pre-Mesozoic succession forming extensional allochthons (Figure 10). It is worth to point out that, although tectonic metabreccia with reworked basement has not been found within the shear zones [124], both in VSZ, SDSZ, and CLSZ tectonic slices of mantle rocks and Variscan basement occur.

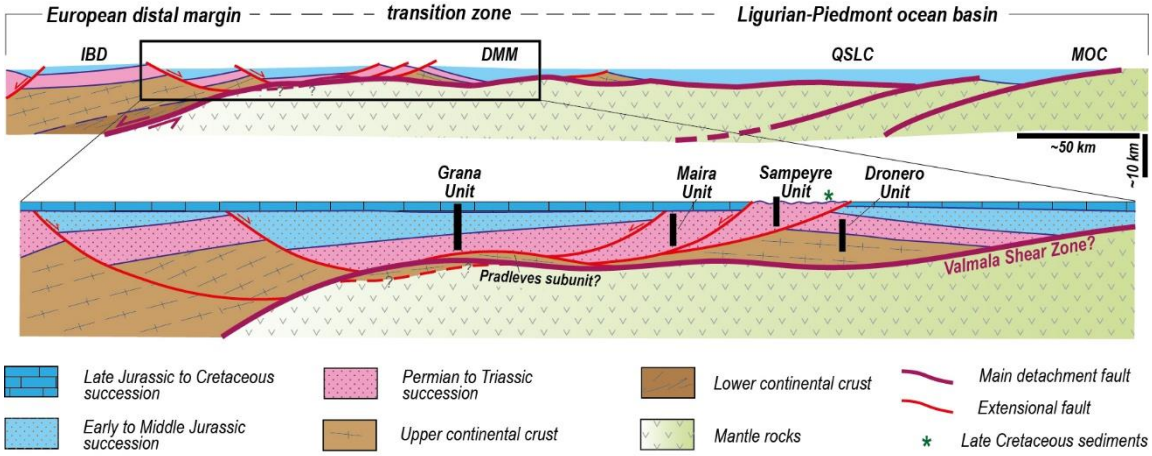

Figure 10. Paleogeographic reconstruction at the Late Jurassic time and detail of the transition zone between the European distal margin and the LPBO (IBD: Internal Briançonnais Domain; DMM: Dora Maira Massif; QSLC: Queyras Schistes Lustrès Complex; MOC: Monviso meta-ophiolite Complex) (modified after [8]).

At the large scale, another possible evidence of the architecture of the European distal margin–Alpine Tethys transition zone is suggested by the occurrence of the tectonic slices of Cambrian (~510 Ma) metadiorite within the VMZ. Rocks with comparable magmatic (protolith) ages have never been described in DMM, wherein dated meta-intrusives are mostly Early Permian in age and, to a lesser extent, Ordovician [50]. The Cambrian metadiorite should be originally part of a Caledonian basement, which seems to be not exposed throughout the tectonic units of the DMM. Notably, a Caledonian basement has been described in the Briançonnais Paleozoic basement of the Ligurian Alps [125]. Although more investigations are needed, if a relatively allochthon basement has been sampled along VMZ (Figure 10), the existence of a main inherited (Jurassic?) structure can be speculated, allowing interpretation of DU (i.e., the hanging wall of the VMZ) as an original extensional allochthon as also supposed for the Brossasco-Isasca Unit by Bonnet et al. (2022) [64].

Our reconstruction of the pre-Alpine tectono-stratigraphic setting of the southwestern Alps allows to highlight the rheological contrasts that controlled the localization of convergent deformation and large-scale basement/cover detachments (the so-called Maira-Sampeyre and Val Grana allochthons [36]). The here described nappe stack allows to detect the main mechanical weaknesses which correspond to (i) the Late Permian fine-grained sediments occurring at the base of SU, (ii) the original gypsum horizons likely occurring at the base of the carbonate platform succession of MU and GU, as also suggested for other Briançonnais units [69,126] and other evaporite rocks [127], (iii) the Middle to Late Jurassic carbonate-siliceous sediments in the uppermost part of the GU succession, and (iv) the Cretaceous sediments now forming QSLC, as also suggested for pelagic shales by Herviou et al., 2022 [128].

7. Conclusions

In the Western Alps, studies about inherited structural settings of distal margin-ocean transition zones are mainly focused on the Adria paleomargin, wherein lithospheric thinning, exhumation of lower crustal, and mantle rocks, as well as the formation of extensional allochthons, are well documented [4]. In this paper, through detailed geological mapping, stratigraphic observations, and U/Pb dating, we document the structural setting of the southern part of Western Alps and the inherited different portions of the so far poorly investigated transition between the European passive margin and the LPBO.

We show that, in the present-day orogen-scale setting, the tectonostratigraphic units are arranged in an upright nappes stack, with the oldest succession at the bottom (the DU) and the youngest one at the top (the QSLC). These successions were sampled from the same basin and are now separated by Alpine shear zones. The finite Alpine deformation recorded by these units decreases from the northeastern sectors, wherein successions are more pervasively folded and sheared, to the southwestern ones, wherein pervasive deformation is mainly localized and primary textures and paleontological contents are partly retained. The Alpine P-T metamorphic peaks seem to follow the same trend, varying from coesite-eclogite facies in northern-eastern sectors to low grade blueschist-facies in southern-western ones [36,63,64,69,82].

In conclusion, the here proposed reconstruction of the pre-Alpine tectono-stratigraphic setting of the southwestern Alps allows us to reveal the existence of an articulated pre-Alpine structural setting of the margin, with inherited faults and structural highs and lows, which had a role as structural inheritances during the Alpine convergence. This study also highlights useful clues for detecting the rheological contrasts, which control the localization of deformation during plate convergence. Mechanical weaknesses within the Late Paleozoic–Late Cretaceous stratigraphic successions strongly constrained the localization, mode, and characteristics of subduction processes (see also Agard, 2021 [8]) and, therefore, the structural evolution at depth.

Supplementary Materials: The following supporting information can be downloaded at: https://www.mdpi.com/article/10.3390/geosciences12100358/s1, Table S1: S1 U-Pb data sample 204; Table S2: S2 U-Pb data sample 1920 [129–133].

Author Contributions: Conceptualization, G.B., A.F., C.G., P.C. and M.R.; methodology, G.B., A.F., C.G., P.C. and M.R.; validation, G.B., A.F., C.G. and P.C.; investigation, G.B., A.F., C.G., P.C. and M.R.; writing—original draft preparation, G.B. and A.F.; writing—review and editing, G.B., A.F., C.G., P.C. and M.R.; supervision, G.B. and A.F.; funding acquisition, A.F. All authors have read and agreed to the published version of the manuscript.

Funding: This research was funded by the University of Torino ("Ricerca Locale ex 60% 2017–2021", grants to A. Festa), and by the Italian Ministry of University and Research (Cofin-PRIN 2020 "POEM project–POligEnetic Mélanges: anatomy, significance and societal impact", grants no. 2020542ET7_003 to A. Festa).

Data Availability Statement: Not applicable.

Acknowledgments: We thank M. Gattiglio for the discussion about geology of the Western Alps, and F. Dela Pierre and R. Gennari for their suggestions about paleontological relicts in our rocks. We also thank P. Adamo, Y. Bagetta, F. Baudana, A. Berloffa, M. Calorio, P. Cavallera, L. Di Martino, F. Nosenzo, A. Pagliero, and L. Pellerey for fieldwork during their Msc Theses. We particularly thank the three referees for their constructive and thorough reviews, from which we have benefited greatly in revising our manuscript.

Conflicts of Interest: The authors declare no conflict of interest.

References

1. Candiotti, L.G.; Duretz, T.; Moulas, E.; Schmalholz, S.M. Buoyancy versus shear forces in building orogenic wedges. *Solid Earth* **2021**, *12*, 1749–1775. [CrossRef]
2. Chenin, P.; Manatschal, G.; Picazo, S.; Müntener, O.; Karner, G.; Johnson, C.; Ulrich, M. Influence of the architecture of magma-poor hyperextended rifted margins on orogens produced by the closure of narrow versus wide oceans. *Geosphere* **2017**, *13*, 559–576. [CrossRef]
3. Pfiffner, O.A. Thick-Skinned and Thin-Skinned Tectonics: A Global Perspective. *Geosciences* **2017**, *7*, 71. [CrossRef]
4. Beltrando, M.; Manatschal, G.; Mohn, G.; Dal Piaz, G.V.; Vitale Brovarone, A.; Masini, E. Recognizing remnants of magma-poor rifted margins in high-pressure orogenic belts: The Alpine case study. *Earth Sci. Rev.* **2014**, *131*, 88–115. [CrossRef]
5. Balestro, G.; Festa, A.; Borghi, A.; Castelli, D.; Gattiglio, M.; Tartarotti, P. Role of Late Jurassic intra-oceanic structural inheritance in the Alpine tectonic evolution of the Monviso meta-ophiolite Complex (Western Alps). *Geol. Mag.* **2018**, *155*, 233–249. [CrossRef]
6. Ballèvre, M.; Manzotti, P.; Dal Piaz, G.V. Pre-Alpine (Variscan) inheritance: A key for the location of the future Valaisan basin (western Alps). *Tectonics* **2018**, *37*, 786–817. [CrossRef]
7. Festa, A.; Balestro, G.; Borghi, A.; De Caroli, S.; Succo, A. The role of structural inheritance in continental break-up and exhumation of Alpine Tethyan mantle (Canavese zone, Western Alps). *Geosci. Front.* **2020**, *11*, 167–188. [CrossRef]
8. Agard, P. Subduction of oceanic lithosphere in the Alps: Selective and archetypal from (slow-spreading) oceans. *Earth Sci. Rev.* **2021**, *214*, 103517. [CrossRef]
9. Wissing, S.B.; Pfiffner, O.A. Numerical models for the control of inherited basin geometries on structures and emplacement of the Klippen nappe (Swiss Prealps). *J. Struct. Geol.* **2003**, *25*, 1213–1227. [CrossRef]
10. Bell, C.; Butler, R.W.H. Platform-basin transitions and their role in Alpine-style collision systems: A comparative approach. *Swiss J. Geosci.* **2017**, *110*, 535–546. [CrossRef]
11. Tavani, S.; Granado, P.; Corradetti, A.; Camanni, G.; Vignaroli, G.; Manatschal, G.; Mazzoli, S.; Muñoz, J.A.; Parente, M. Rift inheritance controls the switch from thin- to thick skinned thrusting and basal décollement re-localization at the subduction-to-collision transition. *Geol. Soc. Am. Bull.* **2021**, *133*, 2157–2170. [CrossRef]
12. Mohn, G.; Manatschal, G.; Masini, E.; Müntener, O. Rift-related inheritance in orogens: A case study from the Austroalpine nappes in Central Alps (SE-Switzerland and N-Italy). *Int. J. Earth Sci.* **2011**, *100*, 937–961. [CrossRef]
13. McCarthy, A.; Chelle-Michou, C.; Müntener, O.; Arculus, R.; Blundy, J. Subduction initiation without magmatism: The case of the missing Alpine magmatic arc. *Geology* **2018**, *46*, 1059–1062. [CrossRef]
14. Dumont, T.; Schwartz, S.; Guillot, S.; Malusà, M.; Jouvent, M.; Moniè, P.; Verly, A. Cross-propagation of the western Alpine Orogen from early to late deformation stages: Evidence from the Internal Zones and implications for restoration. *Earth Sci. Rev.* **2022**, *232*, 104106. [CrossRef]
15. Zucali, M.; Corti, L.; Delleani, F.; Zanoni, D.; Spalla, M.I. 3D reconstruction of fabric and metamorphic domains in a slice of continental crust involved in the Alpine subduction system: The example of Mt. Mucrone (Sesia–Lanzo Zone, Western Alps). *Int. J. Earth Sc.* **2020**, *109*, 1337–1354. [CrossRef]
16. Vialon, P. Etude géologique du massif cristallin Dora-Maira Alpes Cottiennes internes (Italie). *Mém. Lab. Géol. Fac. Sci. Grenoble* **1966**, *4*, 293.
17. Michard, A. Etudes géologiques dans les zones internes des Alpes cottiennes. *CNRS Éditions Paris* **1967**, 447.
18. Piana, F.; Fioraso, G.; Irace, A.; Mosca, P.; d'Atri, A.; Barale, L.; Falletti, P.; Monegato, G.; Morelli, M.; Tallone, S.; et al. Geology of Piemonte region (NW Italy, Alps–Apennines interference zone). *J. Maps* **2017**, *13*, 395–405. [CrossRef]
19. Mohn, G.; Manatschal, G.; Beltrando, M.; Masini, E.; Kusznir, N. Necking of continental crust in magma-poor rifted margins: Evidence from the fossil Alpine Tethys margins. *Tectonics* **2012**, *31*, TC1012. [CrossRef]
20. Decarlis, A.; Manatschal, G.; Haupert, I.; Masini, E. The tectonostratigraphic evolution of distal, hyper-extended magma-poor conjugate rifted margins: Examples from the Alpine Tethys and Newfoundland–Iberia. *Mar. Pet. Geol.* **2015**, *68*, 54–72. [CrossRef]
21. Stampfli, G.M.; Borel, G.D.; Marchant, R.; Mosar, J. Western Alps geological constraints on western Tethyan reconstructions. In: Rosenbaum, G. and Lister, G.S.; Reconstruction of the evolution of the Alpine-Himalayan Orogen. *J. Virtual Explor.* **2002**, *7*, 75–104.
22. Rosenbaum, G.; Lister, G.S. The Western Alps from the Jurassic to Oligocene: Spatio-temporal constraints and evolutionary reconstructions. *Earth Sci. Rev.* **2005**, *69*, 281–306. [CrossRef]
23. Manatschal, M.; Müntener, O. A type sequence across an ancient magmapoor ocean-continent transition: The example of the western Alpine Tethys ophiolites. *Tectonophysics* **2009**, *473*, 4–19. [CrossRef]
24. Roda, M.; Regorda, A.; Spalla, M.I.; Marotta, A.M. What drives Alpine Tethys opening? Clues from the review of geological data and model predictions. *Geol. J.* **2019**, *54*, 2646–2664. [CrossRef]
25. Laubscher, H.P. The arc of Western Alps today. *Eclogae Geol. Helv.* **1991**, *84*, 631–659.
26. Handy, M.R.; Schmid, S.M.; Bousquet, R.; Kissling, E.; Bernoulli, D. Reconciling plate-tectonic reconstructions of Alpine Tethys with the geological–geophysical record of spreading and subduction in the Alps. *Earth Sci. Rev.* **2010**, *102*, 121–158. [CrossRef]
27. Butler, J.P.; Beaumont, C.; Jamieson, R.A. The Alps 1: A working geodynamic model for burial and exhumation of (ultra)high-pressure rocks in Alpine-type orogens. *Earth Planet. Sci. Lett.* **2013**, *377*, 114–131. [CrossRef]
28. Schmid, S.M.; Kissling, E.; Diehl, T.; van Hinsbergen, D.J.J.; Molli, G. Ivrea mantle wedge, arc of the Western Alps, and kinematic evolution of the Alps-Apennines orogenic system. *Swiss J. Geosci.* **2017**, *110*, 581–612. [CrossRef]

29. Coward, M.P.; Dietrich, D. Alpine tectonics—An overview. In *Alpine Tectonics*; Coward, M.P., Dietrich, D., Park, R.G., Eds.; Geological Society London, Special Publications: London, UK, 1989; Volume 45, pp. 1–29.
30. Polino, R.; Dal Piaz, G.V.; Gosso, G. Tectonic erosion at the Adria margin and accretionary processes for the Cretaceous orogeny of the Alps. *Mém. Soc. Géol. France* **1990**, *156*, 345–367.
31. Pfiffner, O.A. Basement-involved thin-skinned and thick-skinned tectonics in the Alps. *Geol. Mag.* **2016**, *153*, 1085–1109. [CrossRef]
32. Dal Piaz, G.V.; Bistacchi, A.; Massironi, M. Geological outline of the Alps. *Episodes* **2003**, *26*, 175–180. [CrossRef] [PubMed]
33. Goffè, B.; Schwartz, S.; Lardeaux, J.M.; Bousquet, R. Metamorphic structure of the western and Ligurian Alps. In: Oberhansli, R. Ed., Explanatory note to the map "Metamorphic structure of the Alps". *Mitt. Österr. Mineral. Ges.* **2004**, *149*, 125–144.
34. Beltrando, M.; Compagnoni, R.; Lombardo, B. (Ultra-) High-pressure metamorphism and orogenesis: An Alpine perspective. *Gondwana Res.* **2010**, *18*, 147–166. [CrossRef]
35. Lardeaux, J.; Schwartz, S.; Tricart, P.; Paul, A.; Guillot, S.; Béthoux, N.; Masson, F. A crustal-scale crosssection of the south-western Alps combining geophysical and geological imagery. *Terra Nova* **2006**, *18*, 412–422. [CrossRef]
36. Michard, A.; Schmid, S.M.; Lahfid, A.; Ballèvre, M.; Manzotti, P.; Chopin, C.; Iaccarino, S.; Dana, D. The Maira-Sampeyre and Val Grana Allochthons (south Western Alps): Review and new data on the tectonometamorphic evolution of the Briançonnais distal margin. *Swiss J. Geosci.* **2022**, *115*, 19. [CrossRef]
37. Ellenberger, F.; Lemoine, M. Le faciès prépiémontais et le problème du passage de la zone du Briançonnais aux schistes lustrés piémontais. *C. R. Soc. Géol. France* **1955**, *1955*, 146–148.
38. Tricart, P.; Lemoine, M. The Queyras ophiolite west of Monte Viso (Western Alps): Indicator of a peculiar ocean floor in the Mesozoic Tethys. *J. Geodyn.* **1991**, *13*, 163–181. [CrossRef]
39. Balestro, G.; Lombardo, B.; Vaggelli, G.; Borghi, A.; Festa, A.; Gattiglio, M. Tectonostratigraphy of the northern Monviso meta-ophiolite complex (Western Alps). *Ital. J. Geosci.* **2014**, *133*, 409–426. [CrossRef]
40. Balestro, G.; Festa, A.; Dilek, Y. Structural Architecture of the Western Alpine Ophiolites, and the Jurassic Seafloor Spreading Tectonics of the Alpine Tethys. *J. Geol. Soc.* **2019**, *176*, 913–930. [CrossRef]
41. Lagabrielle, Y.; Vitale Brovarone, A.; Ildefonse, B. Fossil oceanic core complexes recognized in the blueschist metaophiolites of Western Alps and Corsica. *Earth Sci. Rev.* **2015**, *141*, 1–26. [CrossRef]
42. Festa, A.; Balestro, G.; Dilek, Y.; Tartarotti, P. A Jurassic oceanic core complex in the high-pressure Monviso ophiolite (western Alps, NW Italy). *Lithosphere* **2015**, *7*, 646–652. [CrossRef]
43. Sandrone, R.; Cadoppi, P.; Sacchi, R.; Vialon, P. The Dora-Maira massif. In *Pre-Mesozoic Geology in the Alps*; von Raumer, J.F., Neubauer, F., Eds.; Springer Science and Business Media: New York, NY, USA, 1993; pp. 317–325.
44. Graciansky, P.C.; Roberts, D.G.; Tricart, P. *The Western Alps, from Rift to Passive Margin to Orogenic Belt*; Elsevier: Amsterdam, The Netherlands, 2010; p. 432.
45. Caby, R. Low-angle extrusion of high-pressure rocks and the balance between outward and inward displacements of Middle Penninic units in the Western Alps. *Eclogae Geol. Helv.* **1996**, *89*, 229–267.
46. Wheeler, J. Structural evolution of a subducted continental sliver: The northern Dora Maira massif, Italian Alps. *J. Geol. Soc.* **1991**, *148*, 1101–1113. [CrossRef]
47. Michard, A.; Chopin, C.; Henry, C. Compression versus extension in the exhumation of the Dora-Maira coesite-bearing unit, Western Alps, Italy. *Tectonophysics* **1993**, *221*, 173–193. [CrossRef]
48. Perrone, G.; Eva, E.; Solarino, S.; Cadoppi, P.; Balestro, G.; Fioraso, G.; Tallone, S. Seismotectonic investigations in the inner Cottian Alps (Italian Western Alps): An integrated approach. *Tectonophysics* **2010**, *496*, 1–16. [CrossRef]
49. Michard, A.; Vialon, P. Permo-Trias, Permien s.l. et Permo-Carbonifère metamorphises des Alpes Cottiennes internes: Les facies "Verrucano" et les series volcano-detritiques du Massif Dora-Maira. Symposium sul Verrucano (Pisa, Settembre 1965). *Atti Soc. Toscana Sci. Nat.* **1966**, *135*, 116–135.
50. Bussy, F.; Cadoppi, P. U–Pb zircon dating of granitoids from the Dora-Maira massif (Western Italian Alps). *Schweizer. Mineralog. Petrog. Mitt.* **1996**, *76*, 217–233.
51. Gasco, I.; Gattiglio, M.; Borghi, A. Lithostratigraphic setting and P–T metamorphic evolution for the Dora Maira Massif along the Piedmont zone boundary (middle Susa Valley, NW Alps). *Int. J. Earth Sci.* **2011**, *100*, 1065–1085. [CrossRef]
52. Cadoppi, P.; Camanni, G.; Balestro, G.; Perrone, G. Geology of the Fontane talc mineralization (Germanasca valley, Italian Western Alps). *J. Maps* **2016**, *12*, 1170–1177. [CrossRef]
53. Nosenzo, F.; Manzotti, P.; Poujol, M.; Ballèvre, M.; Langlade, J. A window into an older orogenic cycle: P-T conditions and timing of the pre-Alpine history of the Dora-Maira Massif (Western Alps). *J. Metamorph. Geol.* **2021**, *40*, 789–821. [CrossRef]
54. Manzotti, P.; Schiavi, F.; Nosenzo, F.; Pitra, P.; Ballevre, M. A journey towards the forbidden zone: A new, cold, UHP unit in the Dora-Maira Massif (Western Alps). *Contrib. Mineral. Petrol.* **2022**, *177*, 59. [CrossRef]
55. Borghi, A.; Cadoppi, P.; Porro, A.; Sacchi, R.; Sandrone, R. Osservazioni geologiche nella Val Germanasca e nella media Val Chisone (Alpi Cozie). *Boll. Mus. Reg. Sci. Nat.* **1984**, *2*, 503–530.
56. Avigad, D.; Chopin, C.; Le Bayon, R. Thrusting and extension in the southern Dora-Maira ultra-high pressure massif (Western Alps): View from below the coesite-bearing unit. *J. Geol.* **2003**, *111*, 57–70. [CrossRef]
57. Chopin, C.; Henry, C.; Michard, A. Geology and petrology of the coesite bearing terrain, Dora Maira Massif, Western Alps. *Eur. J. Mineral.* **1991**, *3*, 263–291. [CrossRef]

58. Gebauer, D.; Schertl, H.P.; Brix, M.; Schreyer, W. 35 Ma old ultrahighpressure metamorphism and evidence for very rapid exhumation in the Dora Maira Massif, Western Alps. *Lithos* **1997**, *41*, 5–24. [CrossRef]
59. Compagnoni, R.; Rolfo, F. UHPM units in the Western Alps. *Eur. Mineral. Union Notes Mineral.* **2003**, *5*, 13–49.
60. Ferrando, S.; Groppo, C.; Frezzotti, M.L.; Castelli, D.; Proyer, A. Dissolving dolomite in a stable UHP mineral assemblage: Evidence from Cal-Dol marbles of the Dora-Maira Massif (Italian Western Alps). *Am. Min.* **2017**, *102*, 42–60. [CrossRef]
61. Compagnoni, R.; Rolfo, F.; Groppo, C.; Hirajima, T.; Turello, R. Geologic map of the UHP Brossasco-Isasca Unit (Western Alps). *J. Maps* **2012**, *8*, 465–472. [CrossRef]
62. Henry, C.; Michard, A.; Chopin, C. Geometry and structural evolution of ultra-high pressure and high pressure rocks from the Dora-Maira massif, Western Alps, Italy. *J. Struct. Geol.* **1993**, *15*, 965–981. [CrossRef]
63. Groppo, C.; Ferrando, S.; Gilio, M.; Botta, S.; Nosenzo, F.; Balestro, G.; Festa, A.; Rolfo, F. What's in the sandwich? New P-T constraints for the (U)HP nappe stack of southern Dora-Maira Massif (Western Alps). *Eur. J. Mineral.* **2019**, *31*, 665–683. [CrossRef]
64. Bonnet, G.; Chopin, C.; Locatelli, M.; Kyander-Clark, A.; Hacker, B.R. Protracted subduction of the European hyperextended margin revealed by rutile U-Pb geochronology across the Dora-Maira massif (W. Alps). *Tectonics* **2022**, *41*, e2021TC007170. [CrossRef]
65. Schmid, S.M.; Fügenschuh, B.; Kissling, E.; Schuster, R. Tectonic map and overall architecture of the Alpine orogen. *Ecl. Geol. Helv.* **2004**, *97*, 93–117. [CrossRef]
66. Lefèvre, R.; Michard, A. Les nappes briançonnaises internes et ultrabriançonnaises de la bande d'Acceglio (Alpes franco-italiennes). Une étude structurale et pétrographique dans le faciès des schistes bleus à jadéite. *Sci. Géol. Bull.* **1976**, *29*, 183–222.
67. d'Atri, A.; Piana, F.; Barale, L.; Bertok, C.; Martire, L. Geological setting of the southern termination of Western Alps. *Int. J. Earth Sci.* **2016**, *105*, 1831–1858. [CrossRef]
68. Piana, F.; Barale, L.; Bertok, C.; d'Atri, A.; Irace, A.; Mosca, P. The Alps-Apennines Interference Zone: A Perspective from the Maritime and Western Ligurian Alps. *Geosciences* **2021**, *11*, 185. [CrossRef]
69. Michard, A.; Avigad, D.; Goffé, B.; Chopin, C. The high-pressure metamorphic front of the south Western Alps (Ubaye-Maira transect, France, Italy). *Schweiz. Mineral. Petrogr. Mitt.* **2004**, *84*, 215–235.
70. Ballèvre, M.; Camonin, A.; Manzotti, P.; Poujol, M. A step towards unraveling the paleogeographic attribution of pre-Mesozoic basement complexes in the Western Alps based on U-Pb geochronology of Permian magmatism. *Swiss J. Geosc.* **2020**, *113*, 12. [CrossRef]
71. Franchi, S. Sull'età mesozoica della zona delle pietre verdi nelle Alpi Occiden-tali. *Boll. Com. Geol. It.* **1898**, *35*, 125–179.
72. Sturani, C. Osservazioni preliminari sui calcescisti fossiliferi dell'alta Valgrana (Alpi Cozie meridionali). *Boll. Soc. Geol. Ital.* **1961**, *80*, 225–237.
73. Lombardo, B.; Nervo, R.; Compagnoni, R.; Messiga, B.; Kienast, J.; Mevel, C.; Fiora, L.; Piccardo, G.; Lanza, R. Osservazioni preliminari sulle ofioliti metamorfiche del Monviso (Alpi Occidentali). *Rend. Soc. It. Miner. Petr.* **1978**, *34*, 253–305.
74. Angiboust, S.; Langdon, R.; Agard, P.; Waters, D.; Chopin, C. Eclogitization of the Monviso ophiolite (W. Alps) and implications on subduction dynamics. *J. Metamorph. Geol.* **2012**, *30*, 37–61. [CrossRef]
75. Lombardo, B.; Pognante, U. Tectonic implications in the evolution of the Western Alps ophiolite metagabbros. *Ofioliti* **1982**, *7*, 371–394.
76. Lagabrielle, Y. Ophiolites of the Western Alps and the nature of the Tethyan oceanic lithosphere. *Ofioliti* **1994**, *19*, 413–434.
77. Cordey, F.; Tricart, P.; Guillot, S.; Schwartz, S. Dating the Tethyan Ocean in the Western Alps with radiolarite pebbles from synorogenic Oligocene molasse basins (southeast France). *Swiss J. Geosci.* **2012**, *105*, 39–48. [CrossRef]
78. Balestro, G.; Festa, A.; Dilek, Y.; Tartarotti, P. Pre-Alpine extensional tectonics of a peridotite-localized oceanic core complex in the late Jurassic, high-pressure Monviso ophiolite (Western Alps). *Episodes* **2015**, *38*, 266–282. [CrossRef]
79. Lagabrielle, Y.; Polino, R. Un schéma structural du domaine des Schistes lustrés ophiolitifères au nord-ouest du massif du Mont Viso (Alpes sudoccidentales) et ses implications. *C. R. Acad. Sci. Paris* **1988**, *306*, 921–928.
80. Tricart, P.; Schwartz, S. A north–south section across the Queyras Schistes lustrés (Piedmont zone, western Alps): Syn-collision refolding of a subduction wedge. *Ecl. Geol. Helv.* **2006**, *99*, 429–442. [CrossRef]
81. Agard, P.; Jolivet, L.; Goffe, B. Tectonometamorphic evolution of the Schistes Lustrés complex: Implications for the exhumation of HP and UHP rocks in the western Alps. *Bull. Soc. Géol. France* **2001**, *172*, 617–636. [CrossRef]
82. Schwartz, S.; Guillot, S.; Reynard, B.; Lafay, R.; Nicollet, C.; Debret, B.; Auzende, A.L. Pressure–temperature estimates of the lizardite/antigorite transition in high pressure serpentinites. *Lithos* **2013**, *178*, 197–210. [CrossRef]
83. Michard, A. Schéma structural du massif triasico-liasique Maira-Grana dans ses rapports avec les Schistes Lustrés et le massif Dora-Maira (Alpes-Cottiennes). *C. R. Acad. Sci. Paris* **1961**, *253*, 2726–2728.
84. Cohen, K.M.; Finney, S.C.; Gibbard, P.L.; Fan, J.X. The ICS International Chronostratigraphic Chart. [updated August 2018]. *Episodes* **2013**, *36*, 199–204. [CrossRef] [PubMed]
85. Balestro, G.; Nosenzo, F.; Cadoppi, P.; Fioraso, G.; Groppo, C.; Festa, A. Geology of the southern Dora-Maira Massif: Insights from a sector with mixed ophiolitic and continental rocks (Valmala tectonic unit, Western Alps). *J. Maps* **2020**, *16*, 736–744. [CrossRef]
86. Decarlis, A.; Dallagiovanna, G.; Lualdi, A.; Maino, M.; Seno, S. Stratigraphic evolution in the Ligurian Alps between Variscan heritages and the Alpine Tethys opening: A review. *Earth Sci. Rev.* **2013**, *125*, 43–68. [CrossRef]

87. Petti, F.M.; Furrer, H.; Collo, E.; Martinetto, E.; Bernardi, M.; Delfino, M.; Romano, M.; Piazza, M. Archosauriform footprints in the Lower Triassic of Western Alps and their role in understanding the effects of the Permian-Triassic hyperthermal. *PeerJ* **2020**, *8*, e10522. [CrossRef]
88. Lemoine, M.; Marthaler, M.; Caron, M.; Sartori, M.; Amaudric du Chaffaut, S.; Dumont, T.; Escher, A.; Masson, H.; Polino, R.; Tricart, P. Decouverte de foraminifères planctoniques du Crétacé supérieur dans les Schistes lustrés du Queyras (Alpes Occidentales). Conséquences paléogéographiques et tectoniques. *C. R. Acad. Sci. Paris* **1984**, *299*, 727–732.
89. Marthaler, M.; Fudral, S.; Deville, E.; Rampnoux, J.-P. Mise en évidence du Crétacé supérieur dans la couverture septentrionale de Dora Maira, région de Suse, Italie (Alpes occidentales). Conséquences paléogéographiques et structurales. *C. R. Acad. Sci. Paris* **1986**, *302*, 91–96.
90. Tartarotti, P.; Martin, S.; Festa, A.; Balestro, G. Metasediments Covering Ophiolites in the HP Internal Belt of the Western Alps: Review of Tectono-Stratigraphic Successions and Constraints for the Alpine Evolution. *Minerals* **2021**, *11*, 411. [CrossRef]
91. Vanossi, M. La serie Brianzonese del Salto del Lupo (Liguria Occidentale): Osservazione sedimentologico-stratigrafiche. *Atti Ist. Geol. Univ. Pavia* **1969**, *20*, 3–16.
92. Decarlis, A.; Lualdi, L. Late Triassic-Early Jurassic paleokarst from the Ligurian Alps and its geological significance (Siderolitico Auct., Ligurian Briançonnais domain). *Swiss J. Geosci.* **2008**, *101*, 579–593. [CrossRef]
93. Michard, A.; Sturani, C. Détermination de quelques Céphalopodes, notamment Ammonoidés, dans le dolomites triasique du Val Grana (Alpes Cottiennes méridionales). *C. R. Somm. Sci. Soc. Géol. France* **1963**, *1963*, 11–13.
94. Franchi, S.; Di Stefano, G. Sull'età di alcuni calcari e calcescisti fossiliferi delle valli Grana e Maira nelle Alpi Cozie. *Boll. R. Com. Geol. It.* **1896**, *27*, 171–180.
95. Boni, A.; Cerro, A.; Gianotti, R.; Vanossi, M. Note Illustrative della Carta Geologica d'Italia alla scala 1:100000, Foglio 92-93, Albenga-Savona. *Serv. Geol. It.* **1971**, 142.
96. Ellenberger, F.; Michard, A.; Sturani, C. Découverte d'Ammonites et observations stratigraphiques dans les «Schistes lustrés» du Val Grana (Alpes cottiennes). *C. R. Acad. Sci. Paris* **1964**, *259*, 3047–3050.
97. Decarlis, A.; Lualdi, A. Synrift sedimentation on the northern Tethys margin: An example from the Ligurian Alps (Upper Triassic to Lower Cretaceous, Prepiedmont domain, Italy). *Int. J. Earth Sci.* **2011**, *100*, 1589–1604. [CrossRef]
98. Franceschetti, B. Osservazioni e considerazioni sulle intercalazioni di brecce calcareo-dolomitiche della formazione dei calcescisti nelle Alpi Cozie meridionali (Val Grana e bassa valle Stura di Demonte). *Boll. Soc. Geol. It.* **1961**, *4*, 3–24.
99. Dallagiovanna, G.; Lualdi, A. Le Brecce di Monte Galero: Nuovi dati e interpretazioni. *Mem. Soc. Geol. It.* **1986**, *28*, 409–418.
100. Lemoine, M.; Tricart, P. Les Schistes lustrés piémontais des Alpes occidentales: Approche stratigraphique, structurale et sédimentologique. *Ecl. Geol. Helv.* **1986**, *79*, 271–294.
101. Principi, G.; Bortolotti, V.; Chiari, M.; Cortesogno, L.; Gaggero, L.; Marcucci, M.; Saccani, E.; Treves, B. The pre-orogenic volcano-sedimentary covers of the western Tethys oceanic basin: A review. *Ofioliti* **2004**, *29*, 177–212.
102. Tricart, P.; Lemoine, M. Serpentinite oceanic bottom in South Queyras ophiolites (French Western Alps): Record of the incipient oceanic opening of the mesozoic ligurian Tethys. *Ecl. Geol. Helv.* **1983**, *76*, 611–629.
103. Festa, A.; Meneghini, F.; Balestro, G.; Pandolfi, L.; Tartarotti, P.; Dilek, Y.; Marroni, M. Comparative analysis of the sedimentary cover units of the Jurassic Western Tethys ophiolites in the Northern Apennines and Western Alps (Italy): Processes of the formation of mass transport and chaotic deposits during seafloor spreading and subduction zone tectonics. *J. Geol.* **2021**, *129*, 533–562.
104. Schaaf, A.; Polino, R.; Lagabrielle, Y. Nouvelle découverte de radiolaires d'âge Oxfordien supérieur–Kimméridgien inférieur à la base d'une série supra-ophiolitique des schistes lustrés piémontais (Massif de Traversiera, Haut Val Maira, Italie). *C. R. Acad. Sci. Paris* **1985**, *14*, 1079–1084.
105. De Wever, P.; Danelian, T.; Durand-Delga, M.; Cordey, F.; Kito, N. Datations des radiolarites post-ophiolitiques de Corse alpine à l'aide des Radiolaires. *C. R. Acad. Sci. Paris* **1987**, *305*, 893–900.
106. Baumgartner, P.O.; Bartolini, A.; Carter, E.S.; Conti, M.; Cortese, G.; Danelian, T.; De Wever, P.; Dumitrica, P.; Dumitrica-Jud, R.; Gorican, S.; et al. Middle Jurassic to Early Cretaceous radiolarian biochronology of Tethys based on unitary associations. In *Middle Jurassic to Lower Cretaceous Radiolaria of Tethys: Occurrences, Systematics, Biochronology*; Baumgartner, P.O., O'Dogherty, L., Gorican, S., Urquhart, E., Pillevuit, A., De Wever, P., Eds.; Memoires de Geologie: Lausanne, Switzerland, 1995; Volume 23, pp. 1013–1043.
107. Lemoine, M.; Steen, D.; Vuagnat, M. Sur le problème des ophiolites piémontaises et des roches sédimentaires associées: Observations dans le massif de Chabrière en Haute-Ubaye. *C. R. Acad. Sci. Paris* **1970**, *5*, 44–59.
108. Bonioli, L.; Cadoppi, P.; Sacchi, R. Occurrence of metavolcanics in the southernmost Dora-Maira Massif (Italian Western Alps). In *Contributions to the Geology of Italy with Special Regard to the Paleozoic Basements. A Volume Dedicated to Tommaso Cocozza*; Carmignani, L., Sassi, F.P., Eds.; International Geoscience Programme Council: Padova, Italy, 1992; Volume 276, pp. 237–240.
109. Rossignol, C.; Hallot, E.; Bourquin, S.; Poujol, M.; Jolivet, M.; Pellenard, P.; Ducassou, C.; Nalpas, T.; Heilbronn, G.; Yue, J.; et al. Using volcaniclastic rocks to constrain sedimentation ages: To what extent are volcanism and sedimentation synchronous? *Sediment. Geol.* **2019**, *381*, 46–64. [CrossRef]
110. Chen, Y.X.; Zhou, K.; Zheng, Y.F.; Schertl, H.P. Zircon geochemical constraints on the protolith nature and metasomatic process of the Mg-rich whiteschists from the Western Alps. *Chem. Geol.* **2017**, *467*, 177–195. [CrossRef]
111. White, J.D.L.; Houghton, B.F. Primary volcaniclastic rocks. *Geol. Soc. Am. Bull.* **2006**, *34*, 677–680. [CrossRef]

112. Manville, V.; Németh, K.; Kano, K. Source to sink: A review of three decades of progress in the understanding of volcaniclastic processes, deposits, and hazards. *Sediment. Geol.* **2009**, *220*, 136–161. [CrossRef]
113. Dallagiovanna, G.; Gaggero, L.; Maino, M.; Seno, S.; Tiepolo, M. U–Pb zircon ages for post-Variscan volcanism in the Ligurian Alps (Northern Italy). *J. Geol. Soc.* **2009**, *166*, 101–114. [CrossRef]
114. Cortesogno, L.; Dallagiovanna, G.; Gaggero, L.; Seno, S.; Vanossi, M. Tettonica e vulcanismo tardo-paleozoici nel dominio prepiemontese delle Alpi Liguri: La testimonianza della successione del Colle Scravaion. *Atti. Tic. Sci. Terra* **1998**, *7*, 17–26.
115. Muttoni, G.; Kent, D.V.; Garzanti, E.; Brack, P.; Abrahamsen, N.; Gaetani, M. Early Permian Pangea 'B' to late Permian Pangea 'A'. *Earth Planet. Sci. Lett.* **2003**, *215*, 379–394. [CrossRef]
116. Spalla, M.I.; Zanoni, D.; Marotta, A.M.; Rebay, G.; Roda, M.; Zucali, M.; Gosso, G. The transition from Variscan collision to continental break-up in the Alps: Insights from the comparison between natural data and numerical model predictions. *Geol. Soc. Sp. Publ.* **2014**, *405*, 363–400. [CrossRef]
117. Cassinis, G.; Perotti, C.; Santi, G. Post-Variscan Verrucano-like deposits in Italy, and the onset of the alpine tectono-sedimentary cycle. *Earth Sci. Rev.* **2018**, *185*, 476–497. [CrossRef]
118. Schuster, R.; Stüwe, K. Permian metamorphic event in the Alps. *Geology* **2018**, *36*, 603–606. [CrossRef]
119. Lemoine, M. Données nouvelles sur la série du Gondran près Briançon (Alpes Cottiennes). Réflexions sur les problèmes stratigraphique et paléogéographique de la zone piémontaise. *Géol. Alp.* **1971**, *47*, 181–201.
120. Guillot, S.; Hattori, K.; Agard, P.; Schwartz, S.; Vidal, O. Exhumation processes in oceanic and continental subduction contexts: A review. In *Subduction Zone Geodynamics*; Lallemand, S., Funiciello, F., Eds.; Springer: New York, NY, USA, 2009; p. 275.
121. Tribuzio, R.; Garzetti, F.; Corfu, F.; Tiepolo, M.; Renna, M.R. U–Pb zircon geochronology of the Ligurian ophiolites (Northern Apennine, Italy): Architecture of the Western Alpine Ophiolites. Implications for continental breakup to slow seafloor spreading. *Tectonophysics* **2016**, *666*, 220–243. [CrossRef]
122. Rebay, G.; Zanoni, D.; Langone, A.; Luoni, P.; Tiepolo, M.; Spalla, M.I. Dating of ultramafic rocks from the Western Alps ophiolites discloses Late Cretaceous subduction ages in the Zermatt–Saas Zone. *Geol. Mag.* **2018**, *155*, 298–315. [CrossRef]
123. Bertok, C.; Martire, L.; Perotti, E.; d'Atri, A.; Piana, F. Middle-Late Jurassic syndepositional tectonics recorded in the Ligurian Briançonnais succession (Marguareis–Mongioie area, Ligurian Alps, NW Italy). *Swiss J. Geosci.* **2011**, *104*, 237–255. [CrossRef]
124. Epen, M.E.; Manatschal, G.; Amman, M. Defining diagnostic criteria to describe the role of rift inheritance in collisional orogens: The case of the Err-Platta nappes (Switzerland). *Swiss J. Geosci.* **2017**, *110*, 419–438. [CrossRef]
125. Maino, M.; Gaggero, L.; Langone, A.; Seno, S.; Fanning, M. Cambro-Silurian magmatisms at the northern Gondwana margin (Penninic basement of the Ligurian Alps). *Geosci. Front.* **2018**, *10*, 315–330. [CrossRef]
126. Barré, G.; Strzerzynski, P.; Michels, R.; Guillot, S.; Cartigny, P. Tectono-metamorphic evolution of an evaporitic décollement as recorded by mineral and fluid geochemistry: The "Nappe des Gypses" (Western Alps) case study. *Lithos* **2020**, *358–359*, 105419. [CrossRef]
127. Manatschal, G.; Chenin, P.; Lescoutre, R.; Miró, J.; Cadenas, P.; Saspiturry, N.; Masini, E.; Chevrot, S.; Ford, M.; Jolivet, L.; et al. The role of inheritance in forming rifts and rifted margins and building collisional orogens: A Biscay-Pyrenean perspective. *Bull. Soc. Géol. Fr.* **2021**, *192*, 55. [CrossRef]
128. Herviou, C.; Agard, P.; Plunder, A.; Mendes, K.; Verlaguet, A.; Deldicque, D.; Cubaset, N. Subducted fragments of the Liguro-Piemont ocean, Western Alps: Spatial correlations and offscraping mechanisms during subduction. *Tectonophysics* **2021**, *827*, 229–267. [CrossRef]
129. Petrus, J.A.; Kamber, B.S. VizualAge: A novel approach to laser ablation ICP-MS U-Pb geochronology data reduction. *Geostand. Geoanal. Res.* **2012**, *36*, 247–270. [CrossRef]
130. Paton, C.; Hellstrom, J.C.; Paul, B.; Woodhead, J.D.; Hergt, J.M. Iolite: Freeware for the visualisation and processing of mass spectrometric data. *J. Anal. At. Spectrom.* **2011**, *26*, 2508–2518. [CrossRef]
131. Kramers, J.D.; Tolstikhin, I.N. Two terrestrial lead isotope paradoxes, forward transport modeling, core formation and the history of the continental crust. *Chem. Geol.* **1997**, *139*, 75–110. [CrossRef]
132. Andersen, T. Correction of common lead in U-Pb analyses that do not report 204Pb. *Chem. Geol.* **2002**, *192*, 59–79. [CrossRef]
133. Slama, J.; Kosler, J.; Condon, D.J.; Crowley, J.L.; Gerdes, A.; Hanchar, J.M.; Horstwood, M.S.A.; Morris, G.A.; Nasdala, L.; Norberg, N.; et al. Plesovice zircon—A new natural reference material for U-Pb and Hf isotopic microanalysis. *Chem. Geol.* **2008**, *249*, 1–35. [CrossRef]